

No. 203  
September 1978

INVESTIGATION INTO SHIP MANEUVERABILITY  
IN SHALLOW WATER BY FREE-RUNNING MODEL TESTS

Masataka Fujino

Nabil Daoud

The preparation of this paper  
was supported by a grant  
of the National Science Foundation  
(Grant ENG 76-24588)



Department of Naval Architecture  
and Marine Engineering  
College of Engineering  
The University of Michigan  
Ann Arbor, Michigan 48109

## ABSTRACT

This study concerns the effects of water depth and ship speed on the maneuverability of ships. Free-running experiments were conducted to determine the coefficients and the nonlinear term in Nomoto's expression for the turning rate of a maneuvering ship. The nonlinear term which represents the steady turning characteristic of the ship is determined by the spiral and reversed spiral tests, while the time constants in Nomoto's expression are obtained from the zigzag maneuvers.

The experiments were conducted on an 8 ft model of the supertanker Tokyo Maru at five different water depths of 1.2, 1.5, 2, 3 and 8.7 times the draft. For each water depth, results were obtained at three different speeds of the model.

The results indicate that the course stability of the ship is strongly dependent on the water depth. In particular, the stability decreases as the water depth decreases and it reaches a minimum at a ratio of water depth to draft between 1.5 and 2, then it starts to improve as the water becomes shallower. These findings are in agreement with earlier results obtained by Fujino (1968) using the Captive Model Test technique for the same ship.

The present results also show that the effect of speed on the maneuverability in shallow water is more pronounced at the low speed limit.

## TABLE OF CONTENTS

### Nomenclature

1. Introduction	1
2. Free-Running Model Tests	4
2.1 Model used in the Free-running model tests	4
2.2 Measuring instruments	5
2.3 Analysis of the recorded signals	6
3. Discussions on the Experimental Results	11
4. Conclusions	17
Acknowledgements	18
References	19

## Nomenclature

A	aspect ratio defined by $2T/L$
H	water depth
$I_{zz}$	yaw mass moment of inertia of a ship
$J_{zz}$	yaw added mass moment of inertia of a ship
K	stability index
L	ship's length between perpendiculars
m	mass of a ship
$m_y$	sway added mass of a ship
N	yaw moment
$r (= \dot{\psi})$	yaw angular velocity (turning to starboard is positive)
T	draft of a ship or stability index
$T_1, T_2, T_3$	stability indices
U	advance speed of a ship
Y	sway force
$\beta$	drift angle
$\delta$	rudder angle (rudder deflection to starboard is positive)
$\psi$	heading angle or yaw angle

We shall use the notation:  $Y_\beta = \frac{\partial Y}{\partial \beta}$ ,  $Y_r = \frac{\partial Y}{\partial r}$ ,  $Y_\delta = \frac{\partial Y}{\partial \delta}$ , etc.

## 1. Introduction

It is known that the maneuverability of even a specified ship is not unique but varies according to its loading condition, i.e. ship's draft, trim, etc. Provided that the hull form of a ship is given, it is possible to guess roughly the maneuverability of the ship in a theoretical way even if the method is not completely theoretical but is partly based on the experience. However, when we want to know more definitely and more quantitatively the maneuverability of a specified ship, at present, we cannot help relying on experimental methods.

To investigate the maneuverability of ships experimentally, there exist two ways, one of which is the captive model test and the other is the free-running model test. In the former test, the hydrodynamic force acting on a captive model is measured and then the hydrodynamic derivatives of the maneuvering equations of motion are determined. In the free-running model test, the ship response to the deflection of control surfaces, that is to say, the deflection of rudder in most cases is measured, and the unknown parameters involved in the mathematical model which describes the ship response are determined by making use of the measured response of the ship. By means of the so-called parameter identification, it is possible in principle to determine any number of unknown hydrodynamic derivatives involved in the maneuvering equations of motion by analyzing the maneuvering motion measured during the free-running model tests. However, as far as we can judge from the few known experiences in application of the parameter identification<sup>1,2</sup>, the method is so affected by the noise involved in the measured ship response that it seems to be very difficult to determine the hydrodynamic derivatives of the equations of motion with confidence to the same extent as in the captive model tests.

Hence, in order to determine the unknown parameters of the equations describing the maneuvering motion by the free-running model tests, it is desirable that the mathematical model itself which describes the maneuvering motion is simple, in other words the number of the unknown parameters which should be determined is reduced as much as possible.

Nomoto proposed to describe the yaw response of a ship to rudder deflection by means of the first-order differential equation

$$T\ddot{\psi} + \dot{\psi} = K\delta . \quad (1-1)$$

He also proposed to determine the stability indices  $T$  and  $K$  by analyzing the time history of yaw response to rudder deflection which is measured during a Kempf's zigzag maneuver<sup>3</sup>.

This simplified equation of maneuvering motion has the advantage of a clear description in which the degree of quickness of response and the degree of turning ability are determined by the indices  $T$  and  $K$  respectively. Actually, equation (1-1) can be used successfully to represent the maneuvering motion of ships which are relatively stable on the course.

However, for many ships with large fullness, most of which are unstable on the course, the description of yaw response by means of a first-order differential equation is unsuitable for such an unstable ship. Instead of equation (1-1), second-order differential equations with non-linear term representing the non-linear stationary turning characteristics are proposed by Norrbin<sup>4</sup> and Nomoto<sup>5</sup>:

$$T_1 T_2 \ddot{\psi} + (T_1 + T_2) \dot{\psi} + H(\dot{\psi}) = K\delta + K T_3 \dot{\delta} \quad (1-2)$$

$$T_1 T_2 \ddot{\psi} + (T_1 + T_2) \dot{\psi} + \dot{\psi} + \alpha \dot{\psi}^3 = K\delta + K T_3 \dot{\delta} \quad (1-3)$$

To determine experimentally the parameters  $T_1$ ,  $T_2$  and  $T_3$  involved in the above equations, Bech proposed a technique of phase-plane analysis of Kempf's zigzag maneuver<sup>6</sup>. However, Bech's original method seems to be unreliable because the noise which is unavoidably involved in the measured yaw response, especially signal of yaw rate, make it very difficult to determine the parameters  $T_1$ ,  $T_2$  and  $T_3$  with confidence. In order to remove the defect of Bech's method, Nomoto and others<sup>7</sup> and Fujino<sup>8</sup> have developed modified methods to determine the unknown parameters of equations (1-2) and (1-3) which makes use of phase-plane trajectories as Bech's proposed but reduces the dependence of the computations on noise.

Starting from the non-linear sway and yaw equations which are derived by Taylor's expansion of the hydrodynamic force and moment, Clarke was able to introduce another non-linear mathematical model similar to equations (1-2) and (1-3), and he verified its validity.<sup>9</sup>

In this paper, the authors will use the non-linear mathematical model of equation (1-2) to describe the yaw response of a ship in shallow water, and

will try to determine the unknown parameters involved in the mathematical model by analyzing the results of free-running model tests. Then, the effects of the finite water depth and the advance speed on the maneuvering characteristics will be discussed.

Incidentally, one of the authors studied the shallow-water effects on the hydrodynamic derivatives using the captive model tests and he discussed the maneuverability of ships in shallow water<sup>10</sup>. As stated in the beginning, the maneuvering characteristics of even a certain ship varies remarkably according to its loading condition. However, it is tedious to determine the hydrodynamic derivatives by the captive model test for all of the presumable cases of loading conditions even in one case of water depth; it is also much more tedious to conduct the captive model test for the various cases of other test parameters, for instance, ship's trim, ship speed, etc.

From a practical point of view, it seems to be useful to describe the maneuvering motion with such simplified mathematical models as equations (1-2) and (1-3) even at the cost of accuracy of description, because the unknown parameters of equations (1-2) and (1-3) can be determined by conducting free-running model tests which are easily applicable for full-scale ships. In order that the marine traffic control may function effectively, the traffic controller had better know properly the maneuvering characteristics of an individual ship which will be under his control and the ship navigator on board should know properly the maneuvering characteristics of his own ship. Since the captive model tests cannot comply with such a need, the authors believe that the free-running model tests will become more important.

For these reasons, the authors decided to determine the unknown parameters of the simplified mathematical model (1-2) and then discuss the effects of finite water depth and model speed on the maneuverability in shallow water.

The prototype of the model which was used in the free-running model tests, is a 200,000 DWT oil-tanker. The same ship was also the prototype of a model which one of the authors had used to conduct captive model tests in restricted waters to investigate the effects of restricted waters on the hydrodynamic derivatives. The reason for selecting this particular ship as the prototype in the free-running model tests is that it is necessary to investigate whether or not the extent of the maneuverability of a ship deter-

mined by an experimental method, for instance, the free-running model tests is consistent with that determined by another experimental method, for instance, the captive model tests.

In the free-running model tests, the following experiments were conducted:

- 1) spiral test
- 2) reversed spiral test
- 3) modified zigzag maneuver in which the rudder is switched according to the yaw angular velocity.

Namely, the stationary turning characteristics is determined from 1) the spiral test and 2) the reversed spiral test, and then from 3) the modified zigzag maneuver the time constants  $T_1$ ,  $T_2$  and  $T_3$  are determined.

## 2. Free-Running Model Tests

### 2.1. Model used in the free-running model tests

As stated in the previous chapter, the prototype of the model used in the free-running model tests is a 200,000 DWT oil-tanker; the model is made of plastics reinforced with glass-fiber. The principal particulars and the body plan of the model are shown in Table 1 and Figure 1 respectively. The screw propeller of the model does not exactly correspond to that of the prototype. The geometrical form of a single screw-blade is precisely similar to the prototype, but the number of blades is not the same. Namely, the model propeller has only four blades, although the prototype does have five blades. Hence, the blade area of the model propeller is four fifth of that of the prototype.

The free-running model tests were conducted in the Seakeeping and Maneuvering Tank (100 ft x 60 ft) of the University of Michigan. Since the surface of the bottom floor of the tank was not flat enough for the shallow-water experiments, a new concrete layer was laid on the original floor to improve smoothness of the bottom surface. Consequently, the surface roughness of the bottom was diminished to within  $\pm 2$  millimeters.

The test conditions under which the free-running model tests were conducted are as follows;



water depth/model's draft : 1.2, 1.5, 2.0, 3.0, 8.7  
model speed : 5, 9, 13 knots in full-scale

In what follows, the above-stated three speeds are called "low", "medium" and "high" speeds respectively.

## 2.2 Measuring instruments

The items which were measured at the free-running model tests and the measuring instruments are as follows;

- a) yaw angular velocity ( $\dot{\psi}$ ) ... by rate gyroscope
- b) rudder angle ( $\delta$ ) ..... by potentiometer
- c) model speed (U) ..... by optical tracking apparatus

The model is completely free from the shore, and hence a D.C. motor was installed in it to rotate the screw propeller which was driven by batteries stored inside the model. The number of revolutions of the D.C. motor and the rudder angle were radio-controlled from the shore. A telemetry system, which consists of a transmitter installed inside the model and a receiver set on shore, was used to transmit such measured signals as yaw rate, rudder angle, etc.

The desired model speed stated in the previous section means the advance speed of the model while moving on a straight course, that is to say, approach speed. Hence, once the number of revolutions of the propeller necessary for the model to travel at a desired speed on a straight course was determined, it was fixed during spiral tests, reversed spiral tests and modified zigzag maneuvers at a specified water-depth/model's draft ratio.

Hence, when the model has large sway and yaw motions, for example, in case of the spiral test with a large rudder angle, not only the longitudinal component of the model speed but also the resultant speed of the model were remarkably less than the desired speed.

The calibration of the model speed versus the number of propeller revolutions was conducted by measuring the time interval necessary for the model to travel a prescribed distance under the various constant revolutions of the propeller. In these runs of speed calibration the model was forced to travel as straight as possible by controlling the rudder angle. The pre-

setting of the number of propeller revolutions and the control of the rudder angle were carried out by adjusting the dials on the control console on the shore, which is shown in Photograph 1. As seen in this photograph, this console has some dials by which the number of propeller revolutions, the rudder angle and the direction of propeller revolutions can be selected, and has some analogue meters to display rudder angle, yaw rate and directional angle of the model.

When the model is under voyage, it is tracked by three optical tracking apparatuses (see Photograph 2) which are fixed on the inside wall of the tank. These tracking units are connected directly to a digital computer, which calculates the position of the model and two components of the model speed as well.

The various kinds of measured signals which are transmitted from the model to the receiver on the shore (see Photograph 3) are also fed to the above-mentioned digital computer and stored in the core memory. At the same time, the computer can feed back some processed signals to the control console. By means of this on-line process the directional angle of the model which is obtained by numerical integration of the measured yaw rate can be displayed on the analogue meter of the control console.

All of the measured signals stored in the core memory are transferred to the magnetic disk for the purpose of data preservation. To obtain the phase plane trajectory of the modified zigzag maneuvers, we can take out any pair of two variables, for instance,  $(\dot{\psi}, \ddot{\psi})$  from the magnetic disk and draw the phase plane trajectory on the curve plotter.

The yaw angular acceleration  $\ddot{\psi}$  and the rate of rudder change  $\dot{\delta}$  are computed by numerical differentiation of the yaw angular velocity  $\dot{\psi}$  and the rudder angle  $\delta$  respectively. This numerical differentiation was executed by making use of a numerical differential filter with the cut-off frequency being 1 Hz after Nomoto and others<sup>7</sup>.

### 2.3 Analysis of the recorded signals

Since the test technique and the method of analysis of Dieudonné spiral tests<sup>11</sup> are well known, they will not be discussed in this paper. In what follows, we briefly discuss the reversed spiral tests and the modified zigzag maneuvers.

### 2.3.1 Reversed spiral tests

If a ship is stable on the course, the relationship between the stationary turning rate versus the rudder angle can be obtained throughout the whole range of the rudder angles by conducting Dieudonné spiral tests. On the other hand, if a ship is unstable on the course, the graph of the rudder angle versus the stationary turning rate has a hysteresis loop at the origin of the graph. Hence, it is impossible to determine the detailed relationship between the rudder angle and the turning rate inside the hysteresis loop by Dieudonné spiral tests. To remove this peculiar defect of the spiral tests, Bech introduced the reversed spiral tests<sup>12</sup>. In this method, the rudder angle which gives a specified turning rate is measured and the rudder angle is usually varied periodically so that the yaw rate may vary around a prescribed value. In our experiments, this method, that is to say, the method of periodical changing of the rudder angle was used. A typical example of the record of yaw rate and rudder angle is shown in Figure 2. The mean values of both rudder angle and yaw rate which are needed to draw the rudder angle versus yaw rate relationship, were obtained graphically from the time histories of the two variables  $\dot{\psi}$  and  $\delta$  which were played back on the curve plotter from the magnetic disk. In determining the mean values, we made use of that part of the time histories in which the variation of rudder angle and yaw rate is in a stationarily oscillatory state. In our experiments, after the first three or four oscillations of rudder angle, oscillatory variation of rudder angle and yaw rate reached an almost stationary state. The graphs of the rudder angle versus yaw rate, which will be discussed in the next chapter, are drawn for mean values of the rudder angle  $\delta$  and the yaw rate  $\dot{\psi}$  taken in three or five cyclic variations succeeding such unstationary oscillations as mentioned above. The planimeter was used for the purpose of graphical determination of the mean values.

### 2.3.2 Determination of the time constants $T_1$ , $T_2$ and $T_3$

Since the method to determine the time constants  $T_1$ ,  $T_2$  and  $T_3$  from the modified zigzag maneuvers is explained in detail in reference<sup>13</sup>, only a brief description is given here.

First, we assume that the stationary turning characteristics  $H(\dot{\psi})=K\delta$  is known before the analysis of the modified zigzag maneuver will be started, for instance, as a result of the spiral tests and/or the reversed spiral tests. Then, let both sides of equation (1-2) be multiplied by the variable  $\dot{\psi}$  and let them be integrated with respect to time over an arbitrary interval  $(t_0, t_1)$ ;

$$\frac{T_1 T_2}{K} \int_{t_0}^{t_1} \ddot{\psi} \dot{\psi} dt + \frac{T_1 + T_2}{K} \int_{t_0}^{t_1} \dot{\psi} \ddot{\psi} dt + \frac{1}{K} \int_{t_0}^{t_1} H(\dot{\psi}) \dot{\psi} dt = \int_{t_0}^{t_1} \delta \dot{\psi} dt + T_3 \int_{t_0}^{t_1} \dot{\delta} \dot{\psi} dt \quad (2-1)$$

Alternatively,

$$\frac{T_1 T_2}{K} \int_{\dot{\psi}(t_0)}^{\dot{\psi}(t_1)} \ddot{\psi} d\dot{\psi} + \frac{T_1 + T_2}{K} \int_{\dot{\psi}(t_0)}^{\dot{\psi}(t_1)} \dot{\psi} d\ddot{\psi} + \frac{1}{K} \int_{\psi(t_0)}^{\psi(t_1)} H(\dot{\psi}) d\psi = \int_{\psi(t_0)}^{\psi(t_1)} \delta d\psi + T_3 \int_{\delta(t_0)}^{\delta(t_1)} \dot{\psi} d\delta \quad (2-2)$$

If the above two instants  $t_0$  and  $t_1$  correspond to a single point on the limit cycle of the trajectory drawn on a phase plane, namely

$$\ddot{\psi}(t_0) = \ddot{\psi}(t_1), \dot{\psi}(t_0) = \dot{\psi}(t_1), \psi(t_0) = \psi(t_1), \delta(t_0) = \delta(t_1) \quad (2-3)$$

equation (2-2) reduces to

$$\frac{T_1 T_2}{K} \oint \dot{\psi} d\ddot{\psi} + \frac{1}{K} \oint H(\dot{\psi}) d\psi = \oint \delta d\psi + T_3 \oint \dot{\psi} d\delta \quad (2-4)$$

where the integrals  $\oint \dot{\psi} d\ddot{\psi}$ ,  $\oint H(\dot{\psi}) d\psi/K$ ,  $\oint \delta d\psi$  and  $\oint \dot{\psi} d\delta$  represent the area enclosed by the limit cycle drawn on  $\dot{\psi}$  versus  $\ddot{\psi}$ ,  $H(\dot{\psi})/K$  versus  $\psi$ ,  $\delta$  versus  $\psi$  and  $\dot{\psi}$  versus  $\delta$  phase planes respectively.

Since the state of limit cycle was not attained in most of our modified zigzag maneuvers, equation (2-2) was used for determination of the unknown time constants.

Next, let both sides of equation (1-2) be multiplied by the variable  $\ddot{\psi}$  and let them be integrated with respect to time over the interval  $(t_0, t_1)$ ;

$$\frac{T_1 T_2}{K} \int_{\dot{\psi}(t_0)}^{\dot{\psi}(t_1)} \ddot{\psi} d\dot{\psi} + \frac{T_1 + T_2}{K} \int_{\dot{\psi}(t_0)}^{\dot{\psi}(t_1)} \dot{\psi} d\dot{\psi} + \frac{1}{K} \int_{\dot{\psi}(t_0)}^{\dot{\psi}(t_1)} H(\dot{\psi}) d\dot{\psi} = \int_{\dot{\psi}(t_0)}^{\dot{\psi}(t_1)} \delta d\dot{\psi} + T_3 \int_{\dot{\psi}(t_0)}^{\dot{\psi}(t_1)} \dot{\delta} d\dot{\psi} \quad (2-5)$$

If two instants,  $t_0$  and  $t_1$ , satisfy the conditions (2-3), equation (2-5) reduces to

$$\frac{T_1 + T_2}{K} \oint \dot{\psi} d\dot{\psi} = \oint \delta d\dot{\psi} + T_3 \oint \dot{\delta} d\dot{\psi} \quad (2-6)$$

where the integrals  $\oint \dot{\psi} d\dot{\psi}$ ,  $\oint \delta d\dot{\psi}$  and  $\oint \dot{\delta} d\dot{\psi}$  represent the area enclosed by the limit cycle drawn on  $\dot{\psi}$  versus  $\ddot{\psi}$ ,  $\dot{\psi}$  versus  $\delta$  and  $\dot{\psi}$  versus  $\dot{\delta}$  phase planes respectively. Here, the following relations should be noted;

$$\oint \dot{\psi} d\ddot{\psi} = -\oint \ddot{\psi} d\dot{\psi}, \quad \oint \dot{\psi} d\delta = -\oint \delta d\dot{\psi} \quad (2-7)$$

Since the phase plane trajectory did not draw a limit cycle except in a few cases, as stated already, equation (2-5) was used to determine the time constants.

Apparently, equations (2-2) and (2-5) are two algebraic equations in the three unknowns  $T_1 T_2 / K$ ,  $(T_1 + T_2) / K$  and  $T_3$  since the various integrals included in those equations can be determined by fixing the time interval  $(t_0, t_1)$ . Consequently we must provide more equations in order to solve for the unknowns  $T_1 T_2 / K$ ,  $(T_1 + T_2) / K$  and  $T_3$ . These equations can be obtained by changing the time interval  $(t_0, t_1)$  or by conducting modified zigzag maneuvers with different combinations of the rudder angle and the switching yaw angular velocity. In our experiments, modified zigzag maneuvers were conducted for different combinations of the rudder angle and the switching yaw angular velocity. Besides, the time interval  $(t_0, t_1)$  as well was varied for a single modified zigzag maneuver in order to provide as many equations (2-2) and (2-5) as possible, which were solved by the least square method. Since  $K$  index which represents the turning ability of a ship can be determined from the slope of a straight line which approximates the stationary turning characteristics at small rudder angles, the time constants  $T_1$  and  $T_2$  can be determined from  $T_1 T_2 / K$  and  $(T_1 + T_2) / K$ .

Detailed explanation on how to obtain the phase plane trajectories seems unnecessary except for the  $H(\dot{\psi})/K$  versus  $\psi$  trajectory. Namely, in order to draw the phase plane trajectories except for the  $H(\dot{\psi})/K$  versus  $\psi$  trajectory, it is enough to take out two signals simultaneously, for instance,  $\dot{\psi}$  and  $\ddot{\psi}$  from the disk memory and plot a point  $(\dot{\psi}, \ddot{\psi})$  on a graph with  $\dot{\psi}$  and  $\ddot{\psi}$  being the coordinate axes to obtain the  $\dot{\psi}$  versus  $\ddot{\psi}$  phase plane trajectory.

In what follows, the process of drawing the  $H(\dot{\psi})/K$  versus  $\psi$  trajectory will be briefly described.

First, we draw the stationary turning characteristics, that is to say,  $\delta=H(\dot{\psi})/K$  on the  $\psi$  versus  $\dot{\psi}$  phase plane as shown in Figure 3. Then, the  $H(\dot{\psi})/K$  versus  $\psi$  trajectory is obtained in the following way:

- i) First, let us draw a straight line through a certain point, for instance A on the  $\psi$  versus  $\dot{\psi}$  trajectory parallel to the abscissa or  $\psi$ -axis and let it intersect both  $\dot{\psi}$ -axis and  $\delta=H(\dot{\psi})/K$  curve at two points which are denoted by B and C respectively.
- ii) Next, let us draw another straight line through the point A so that it crosses the  $\psi$ -axis at a right angle and let D denote this cross-point. Then, we define a point E on this perpendicular so that the distance  $\overline{ED}$  may be equal to the distance  $\overline{BC}$ .
- iii) By connecting the points E obtained successively in this manner, we get the desired  $\psi$  versus  $H(\dot{\psi})/K$  trajectory.

In Figure 4, the various phase plane trajectories which are necessary for the above-stated phase plane analysis are shown as an example. The points marked by 1 to 9 in each of those figures correspond to each other and the numbering order of these points, namely, from 1 to 9 coincides exactly with the order of time elapse on the trajectory. In this example,  $(t_1, t_4)$ ,  $(t_2, t_3)$ ,  $(t_2, t_7)$ ,  $(t_2, t_9)$ ,  $(t_4, t_6)$  and  $(t_5, t_8)$  are the time intervals over which the various integrals occurring in equations (2-2) and (2-5) were computed.

### 3. Discussions on the Experimental Results

The stationary turning characteristics of the model which were obtained from the spiral tests and the reversed spiral tests are shown in Figures 5 to 19, in which the ordinate stand for the stationary turning rate  $\dot{\psi}_{t=\infty}$  and the abscissa represents the rudder angle. In each figure, the black circles and the white circles are the  $\dot{\psi}_{t=\infty}$  versus  $\delta$  points obtained from the spiral tests and the reversed spiral tests respectively, and it appears that both kinds of tests can be represented by a single smooth curve. In particular, it should be noted that the stationary turning rates  $\dot{\psi}_{t=\infty}$  which are obtained by the spiral tests and the reversed spiral tests for a certain rudder angle coincide with each other as shown in Figures 8 (see the points for  $\delta: -9^\circ$ ), 12 ( $\delta: 5^\circ$ ), 14 ( $\delta: -9^\circ$ ) and 19 ( $\delta: 10^\circ$  and  $\delta: -13^\circ$ ). These facts indicate that the results of both the spiral tests and reversed spiral tests are reasonable.

In each of Figures 5 to 19, a solid line is drawn as the mean line connecting smoothly both the black circles and the white ones. From the inclination of a straight line tangent to the mean line at the origin, Nomoto's K index is obtained and is shown in Figure 20 as a function of the water-depth/draft ratio. The figure shows that the manner in which the K index varies with the water depth is almost similar in the three cases of the model speed. Namely, as the water depth decreases, the K value increases and it attains the maximum in a region of the water depth where the water-depth/draft ratio ranging from 1.5 to 2.0. However, when the water depth decreases furthermore, the K index begins to decrease very fast. Consequently, the K index at the water-depth/draft ratio, H/T, equal to 1.2 is less than that at H/T ratio equal to 8.7.

Translated in terms of the course stability, what we stated above can be explained as follows: The course stability of the model is positive in the waterway with the H/T ratio being equal to 8.7, and it decreases with decrease of the water depth. After the course stability becomes worst at a certain water depth, where the water-depth/draft ratio being between 1.5 and 2.0, it recovers remarkably as the water depth becomes shallower. In the waterway with H/T equal to 1.2, the course stability is considerably better than in deep water. Hence, it is obvious that the water depth has remarkable influence on the course keeping quality of a ship.

The above-mentioned qualitative conclusion is consistent with what one of the authors found earlier concerning the shallow-water effects on the course stability of a ship which was based on the experimental results of the hydrodynamic derivatives obtained by the planar motion mechanism<sup>10</sup>.

In the captive model tests, it was concluded that the course stability of the same ship became negative when the water-depth/draft ratio was between 1.6 to 2.6. However, the free running model tests do not indicate that the ship becomes unstable in any region of the water depth, but they indicate that the course stability becomes worst in almost the same region of the water depth as the "unstable" region revealed by the captive model tests.

One of the probable reasons why the free running model tests differ from the captive model tests in estimating the course stability of this particular ship is the difference of the slip stream behind the propeller due to the difference in the number of the propeller blades. Because the rudder which is placed in the slip stream of the propeller acts as a stabilizing fin. Another probable reason for the discrepancy is due to the different trailing wakes shed behind the model in the two experiments. In shallow waters, the vorticity shed from the trailing edge of the hull becomes important due to the blockage of the bottom and the tendency of the fluid to flow around the hull. Therefore, the difference in the nature of the vortex sheets shed behind the model in the two experiments will contribute significantly to the resulting hydrodynamic forces and moments acting on the model and consequently on the response of the models. Further developments of this problem are underway at the present time.

In Figure 21, the time constant  $T_1$  which was determined by the phase plane analysis of the modified zigzag maneuvers is shown as a function of the water depth.\*

---

\* Although the physical meanings of the time constants  $T_1$  and  $T_2$  involved in equation (1-2), for instance, are identical, the following convention is used to distinguish between these two time constants in this paper: if  $T_1$  and  $T_2$  are both real and positive, the larger is denoted by  $T_1$  and if one of them is positive and the other is negative, the negative value is denoted by  $T_1$ . Following this convention, the extent of the course stability of a ship can be represented by the time constant  $T_1$ .



Obviously, the qualitative dependence of  $T_1$  value on the water depth agrees well with that of K index. Namely,  $T_1$  value increases with decrease of the water depth, and it attains the maximum at a certain water depth, where the water-depth to draft ratio is between 1.5 and 2. When the water depth becomes shallower,  $T_1$  value tends to decrease so fast that  $T_1$  value at the water-depth/draft ratio equal to 1.2 is considerably less than that at the water-depth/draft ratio equal to 8.7.

In terms of the quickness of yaw response of a ship, the above description can be expressed as follows: First, the quickness of yaw response becomes worse as the water depth decreases. At a certain water depth, the quickness of yaw response becomes worst, and then it recovers so fast that it is remarkably better at H/T equal to 1.2 than in deep water. Hence, it is obvious that the dependences of the maneuvering characteristics of a ship on the water depth as shown in Figures 20 and 21 respectively are completely consistent with each other.

Here, it should be mentioned that more than one point for H/T ratio in Figure 21 are what were obtained by different modified zigzag maneuvers or by different choice of the time interval over which the integrals involved in equations (2-2) and (2-5) should be computed.

In order to investigate whether the effects of shallow water on the maneuverability depends also on the advance speed of a ship, the K index and the time constant  $T_1$ , which are shown in Figure 20 and 21 respectively, are plotted again in an alternative way as shown in Figure 22, in which the ordinate and the abscissa stand for the inverses of  $T_1$  and K respectively. The numbers written beside each group consisting of a few points, indicate the water-depth/draft ratios corresponding to that group. In Figure 22, it is interesting to note that except for the points corresponding to the case of H/T=1.2 and "low" speed, the  $1/T_1$  versus  $1/K$  relationship can be roughly represented by a straight line through the origin. This approximation can be explained as follows: It is well known that the course stability and the turning ability of a ship are two properties which act contrary to each other. Namely, if the  $T_1$  value decreases and hence the ship becomes more stable on the course, K value increases and the turning ability of the ship becomes worse; and vice versa. Moreover, under the assumption that the maneuvering

motion is so small that the linear approximation may be valid for the description of the maneuvering motion, the ratio of  $T_1$  value to  $K$  index can be approximated as follows:

$$\begin{aligned} \frac{T_1}{K} &\approx \frac{T_1+T_2}{K} = \frac{(m+m_y)N_r - Y_\beta(I_{zz}+J_{zz}) - N_\beta^* (-m\bar{U}+Y_r) - N_\beta Y_r^*}{-Y_\beta N_\delta + Y_\delta N_\beta} \\ &\approx \frac{(m+m_y)N_r - Y_\beta(I_{zz}+J_{zz})}{-Y_\beta N_\delta + Y_\delta N_\beta} \end{aligned} \quad (3-1)$$

because  $|T_1| \gg |T_2|$  is true in most cases.

Hence, the change of  $T_1/K$  ratio due to the change of the water depth can be predicted by the shallow-water effects on the hydrodynamic derivatives. As verified by the theory and by the experiments, except for the rudder derivatives  $Y_\delta$  and  $N_\delta$ , the hydrodynamic derivatives tends to increase monotonously as the water depth decreases. Roughly speaking, the shallow-water effects on the various hydrodynamic derivatives do not differ so much. For instance, according to Newman's theory<sup>14</sup>, the shallow-water effects on sway added mass, yaw added mass moment of inertia, lateral force and yaw moment of a rectangular flat plate are identical at the limit when the aspect ratio of the plate,  $A$ , which is defined by  $2T/L$ , goes to zero. Namely,

$$\begin{aligned} \lim_{A \rightarrow 0} \frac{F_i(A, H)}{F_i(A, \infty)} &= \lim_{A \rightarrow 0} \left[ A \frac{T}{H} \beta_i^{-1} - \frac{\pi^2 \left(\frac{T}{H}\right)^2}{8 \log \left( \cos \frac{\pi T}{2H} \right)} \right]^{-1} \\ &= - \frac{8 \log \left( \cos \frac{\pi T}{2H} \right)}{\pi^2 \left(\frac{T}{H}\right)^2} \end{aligned} \quad (3-2)$$

where the subscript  $i$  indicates

$$F_i \equiv (m_y, J_{zz}, Y, N)$$

$$\beta_i = (1, 3/8, 4, 2)$$

On the other hand, the rudder effectiveness in shallow water is affected by various factors, for example, the wake behind a ship, the strength of the slip stream of the propeller which should overcome the resistance increase in

shallow water, the so-called wall effects on the rudder which acts as a lifting surface, etc. Hence, the precise prediction of the shallow-water effects on the rudder derivatives  $Y_\delta$  and  $N_\delta$  seems very difficult. According to Hess's analysis<sup>15</sup>, who computed approximately the shallow-water effects on the rudder effectiveness by considering the rudder as a trailing-edge flap, the shallow-water effects on the derivatives  $Y_\delta$  and  $N_\delta$  are not so simple to consider as in the case of the other hydrodynamic derivatives. For instance, the graph for the ratio of  $Y_\delta$  at a finite water depth to that in deep water has a dip near  $H/T \approx 2.5$  in the case of the example shown by Hess. Also for  $H/T \leq 1.25$ , there exists a strong influence of shallow-water on the rudder derivatives  $Y_\delta$  and  $N_\delta$ . Namely, the derivative  $Y_\delta$  increases remarkably as the water depth decreases, but on the other hand, the derivative  $N_\delta$  decreases.

Roughly speaking, however, the rudder derivatives can be considered almost constant for  $H/T \geq 1.3$ .

Therefore, rough estimation indicates that the right hand side of equation (3-1) does not change so much with the water depth. In reality, the values of  $(T_1 + T_2)/K$  determined by solving the set of linear algebraic equations (2-2) and (2-5) were almost constant not only in both cases of "high" and "medium" speeds but also in "low" speed except for the case of  $H/T = 1.2$ .

For the sake of comparison, the inverses of  $T_1$  and  $K$  which are computed by using the hydrodynamic derivatives measured in the captive model tests are plotted in Figure 22. We note that although the captive model tests were conducted at 12 knots in full-scale, the results of the captive model tests qualitatively agree well with those of the free running model tests at 13 knots in full-scale.

Figure 23 is an alternative representation of Figure 22. Both axes stand for the inverses of non-dimensional  $T'_1$  and  $K'$  indices:

$$\frac{1}{T'_1} = \frac{1}{T} \frac{L}{U}$$

$$\frac{1}{K'} = \frac{1}{K} \frac{U}{L}$$

(3-3)

If the hydrodynamic forces acting on the hull and the rudder are proportional to the square of ship speed,  $1/T'_1$  value should be described as an

unique function of  $1/K'$  irrespective of the ship speed. Actually, the data for "high" speed and "medium" speed can be approximately described by a single curve, but the data for "low" speed deviate from the curve.

Finally, let us reconsider the method to determine  $T_1 T_2 / K$ ,  $(T_1 + T_2) / K$  and  $T_3$ , which were determined in this paper by solving the set of equations (2-2) and (2-5). As a matter of fact, the set of more than two equations (2-2) and (2-5), which were prepared not only by conducting modified zigzag maneuvers for different pairs of the rudder angle and the switching yaw angular velocity but also by using the various time intervals,  $(t_0, t_1)$ , for a single modified zigzag maneuver, were solved by the least square method in order to determine the unknowns with high confidence. However, when the choice of the combination of the rudder angle and the switching yaw angular velocity or the choice of the time intervals was inadequate, the matrix of the coefficients of the set of equations (2-2) and (2-5) tend to become nearly singular and it was difficult to solve the equations with confidence. In reality, the solution for  $T_1 T_2 / K$  was less accurate than the other unknowns in most cases, and in few cases we obtained unreasonable solutions mainly for  $T_1 T_2 / K$ .

It appears that we must use some different methods to avoid this difficulty. Of course, conducting the modified zigzag maneuvers with considerably different combinations of the rudder angle and the switching yaw angular velocity is one of the probable solutions, but it seems tedious.

An alternative way is to add another equation with the unknowns  $T_1 T_2 / K$ ,  $(T_1 + T_2) / K$  and  $T_3$  to the set of algebraic equations to be solved. For example, let both sides of equation (1-2) be multiplied by the variable  $\psi$  and let them be integrated over the interval  $(t_0, t_1)$ :

$$\frac{T_1 T_2}{K} \int_{t_0}^{t_1} \ddot{\psi} \psi dt + \frac{T_1 + T_2}{v} \int_{t_0}^{t_1} \dot{\psi} \psi dt + \frac{1}{K} \int_{t_0}^{t_1} H(\dot{\psi}) \psi dt = \int_{t_0}^{t_1} \delta \psi dt + T_3 \int_{t_0}^{t_1} \dot{\delta} \psi dt \quad (3-4)$$

Then, it is possible to determine three unknowns by solving the set of linear algebraic equations (2-2), (2-5) and (3-4). The integrals  $\int H(\dot{\psi}) \psi dt / K$  and  $\int \psi \delta dt$  should be obtained by a straightforward integration with respect to

the time, and moreover it should be noted that before the modified zigzag maneuver is started, the ship's heading angle should be carefully kept as straight as possible by deflecting the rudder. Needless to say, the variable  $\psi$  appearing in equation (3-4) stands for the heading angle by which a ship deviates from the approach heading angle.

In the present analysis of the modified zigzag maneuvers, this method was not tried because care to keep the model on a straight course during the approach was not taken in the experiments.

#### 4. Conclusions

With the model of an oil-tanker, of which the hydrodynamic derivatives in shallow water were measured several years ago, the free running model tests, namely, the spiral tests, the reversed spiral tests and the modified zigzag maneuvers were conducted in order to investigate the influence of both ship speed and shallow water on ship maneuverability. The main conclusions obtained by this investigation are as follows:

- i) The course stability of a ship is remarkably dependent on the water depth. Namely, our model which is stable on the course in deep water has the minimum course stability for  $1.5 \leq H/T \leq 2.0$ . However, in shallower water, for example, at the water depth where the water-depth/draft ratio being equal to 1.2, the model is remarkably stable than in deep water.
- ii) The shallow-water effects on ship maneuverability obtained by the present free running model tests qualitatively agree well with those deduced from the captive model tests. Hence, although the maneuvering characteristics determined by the free running model tests differ quantitatively from those obtained by the captive model tests, we can conclude that the free running model tests yield predictions of the shallow-water effects which are consistent with that based on the captive model tests.
- iii) The present results also show that the maneuverability in shallow water at "low" speed is different from that at "medium" and "high" speed.
- iv) As a problem to be solved in the future, the method to determine the time constants from the phase plane analysis of the modified

zigzag maneuvers should be improved.

Acknowledgements

The authors are indebted to many people for their cooperation, useful discussions and assistance, and hence we wish to express our appreciation to:

Prof. T. F. Ogilvie

Mr. V. Phelps

Prof. R. Keller

Dr. V. Leipa

Mr. J. Foulke

Mrs. S. Atkins

Mr. C. Cary

Mr. G. Petrie

This work was financially supported by the National Science Foundation.

## References

- 1) Nonaka, K., "Determination of Hydrodynamic Coefficients from Free-Sailing Model Tests," 20th Seminar in Ship Research Institute, 1970 (in Japanese).
- 2) Kaplan, P. and others, "The Application of System Identification to Dynamics of Naval Craft," 9th Symposium on Naval Hydrodynamics, 1972.
- 3) Nomoto, K., "Analysis of Kempf's Standard Maneuver Test and Proposed Steering Quality Indices," 1st Symposium on Ship Maneuverability, David Taylor Model Basin Report No. 1461, 1960.
- 4) Norrbin, N.H., "Zig-Zag-Proveto Teknik och Analys," Allmän Rapport från SSPA, 1965.
- 5) Nomoto, K., "Approximate Non-Linear Analysis on Steering Motion," Proc. of 12th I.T.T.C., 1969.
- 6) Bech, M. and Smitt, L.W., "Analogue Simulation of Ship Manoeuvres Based on Full-Scale Trials of Free-Sailing Model Tests," Hydro- and Aerodynamic Laboratory Report No. Hy-14, 1969.
- 7) Nomoto, K., Kose, K. and Yoshimura, Y., "A New Procedure of Analysing Zig-Zag Test," Journal of the Society of Naval Architects of Japan, Vol. 134, 1973 (in Japanese).
- 8) Fujino, M., "An Analyzing Method of Manoeuvrability with the Phase Portrait," Journal of the Society of Naval Architects of Japan, Vol. 132, 1972 (Part 1), Vol. 134, 1973 (Part 2).
- 9) Clarke, D., "A New Non-Linear Equation for Ship Manoeuvring," International Shipbuilding Progress, Vol. 18, No. 201, 1971.
- 10) Fujino, M., "Experimental Studies on Ship Manoeuvrability in Restricted Waters," International Shipbuilding Progress, Vol. 15, No. 168 (Part 1), 1968.
- 11) Dieudonné, J., "Note sur la Stabilité du Régime de Route de Navires," Association Technique Maritime et Aeronautique, Session 1949.
- 12) Bech, M., "The Reversed Spiral Tests as Applied to Large Ships," Shipping World, Nov., 1968.
- 13) Fujino, M., "Maneuverability in Restricted Waters: State of the Art," Dept. of Naval Architecture and Marine Engineering, The University of Michigan, Report No. 184, 1976.
- 14) Newman, J.N., "Lateral Motion of a Slender Body Between Two Parallel Walls," Journal of Fluid Mechanics, Vol. 39, 1969.
- 15) Hess, F., "Rudder Effectiveness and Course-Keeping Stability in Shallow Water: A Theoretical Model," (unpublished), 1977.

Table 1. Principal particulars of the model

Length between perpendiculars (L)	2.4383 m (8 ft)
Moulded breadth (B)	0.3994 m
Moulded draft (even keel) (T)	0.1345 m
Displacement	105.83 kg
Block coefficient	0.8054
Longitudinal center of buoyancy	0.0621 m fore from midship
Radius of gyration	0.269 L
Rudder area	5040.1 mm <sup>2</sup>
Diameter of propeller	65.59 mm
Pitch ratio	0.7397
Boss ratio	0.1821
Direction of rotation	right
Rake angle	7°01'
Number of blades	4*
Scale	1/118.9

\* The propeller of the prototype ship has five blades. Hence the blade area of the model is four fifth of that of the prototype.



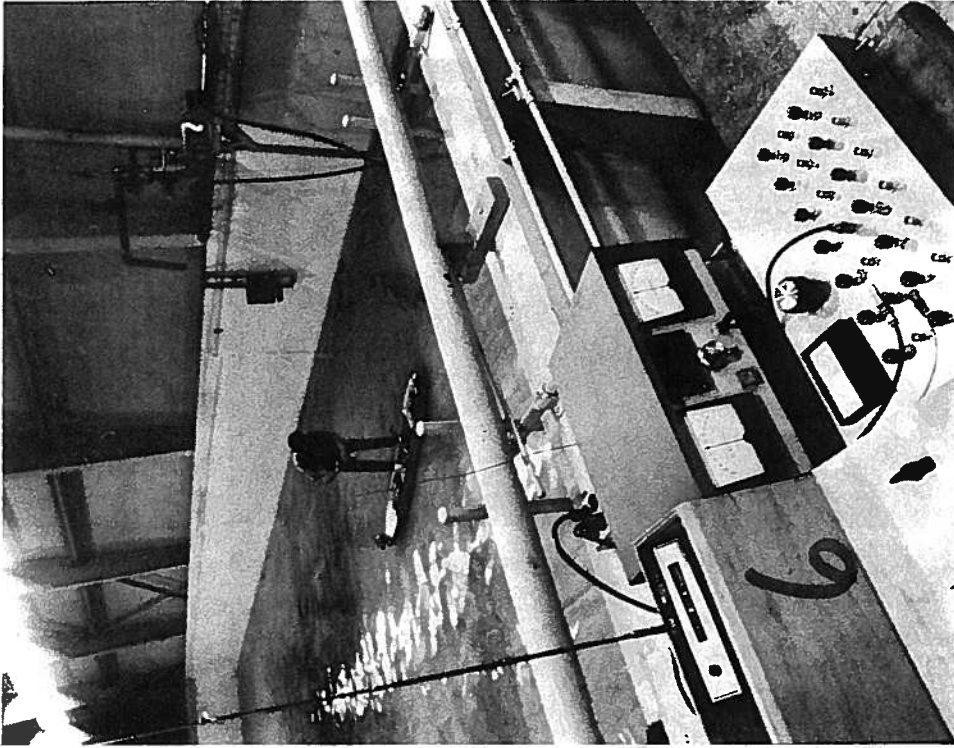


Photo 2. The black box, which is seen on the right of a man standing beside the model, is one of the optical tracking apparatus.

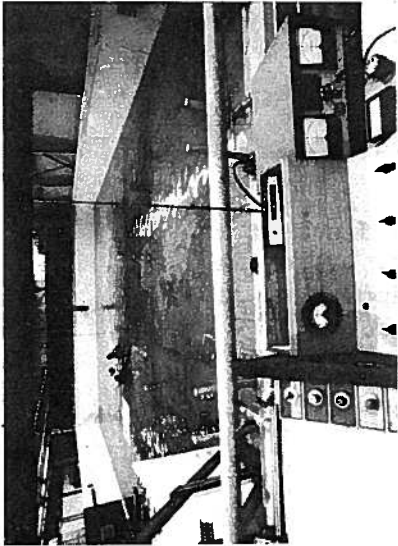


Photo 1. The center of three consoles (which are) set on this side of the tank is the control console. It has four dials for setting the number of propeller revolution, etc.

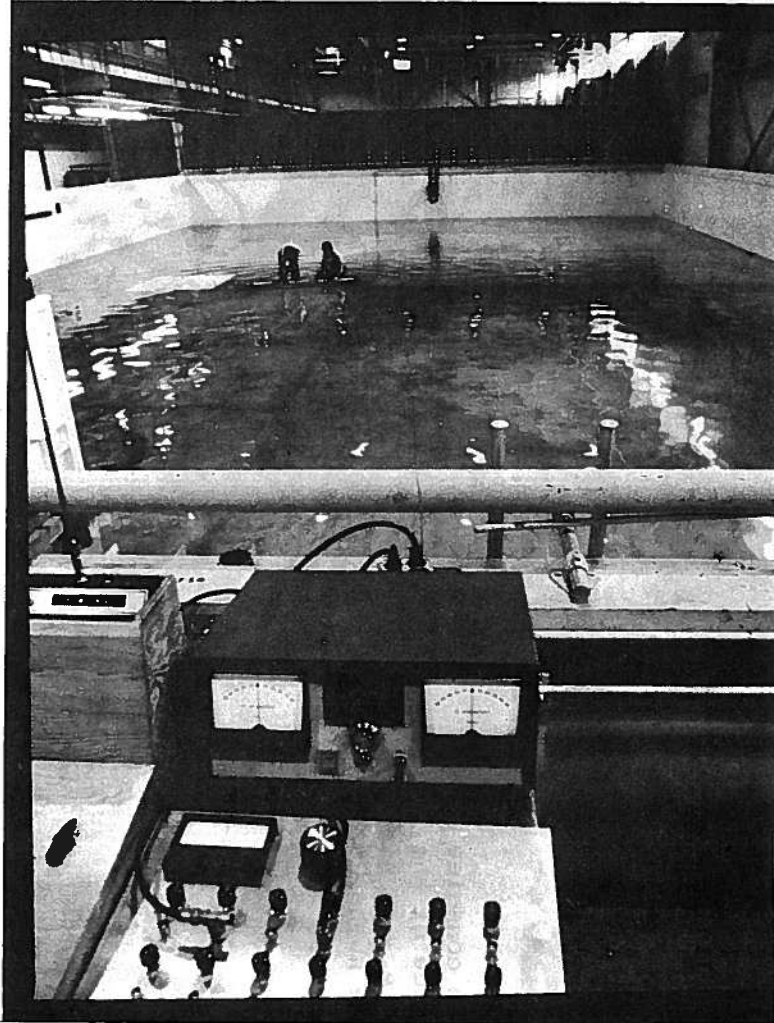
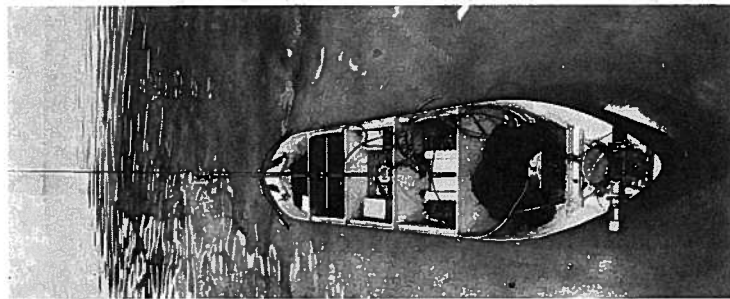
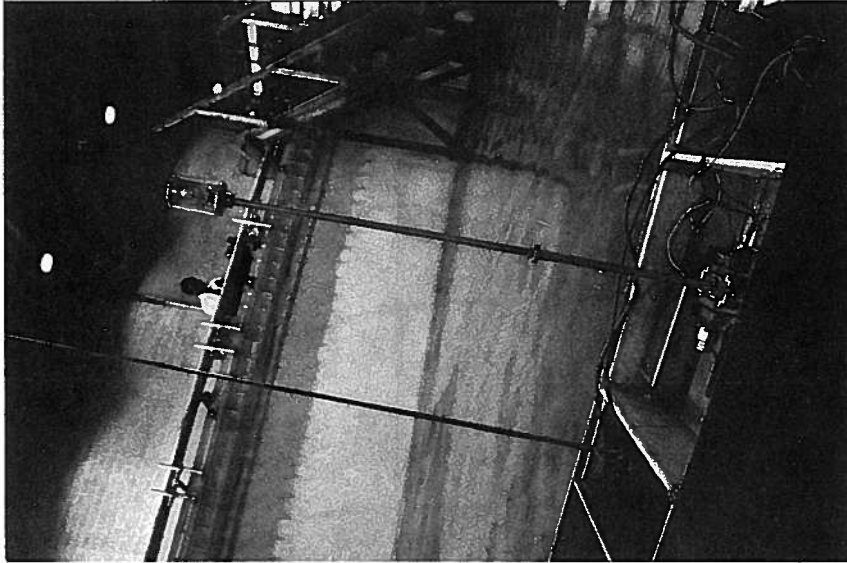


Photo 3. The dark box in the front of the photo is the receiver unit. Also, we can see another tracking apparatus fixed on the far wall of the tank.



(a)



(b) The left pole is the antenna of the telemetry and on the top of the right pole a light for optical tracking is installed inside the transparent plastics.

Photo 4. Inside view of the model

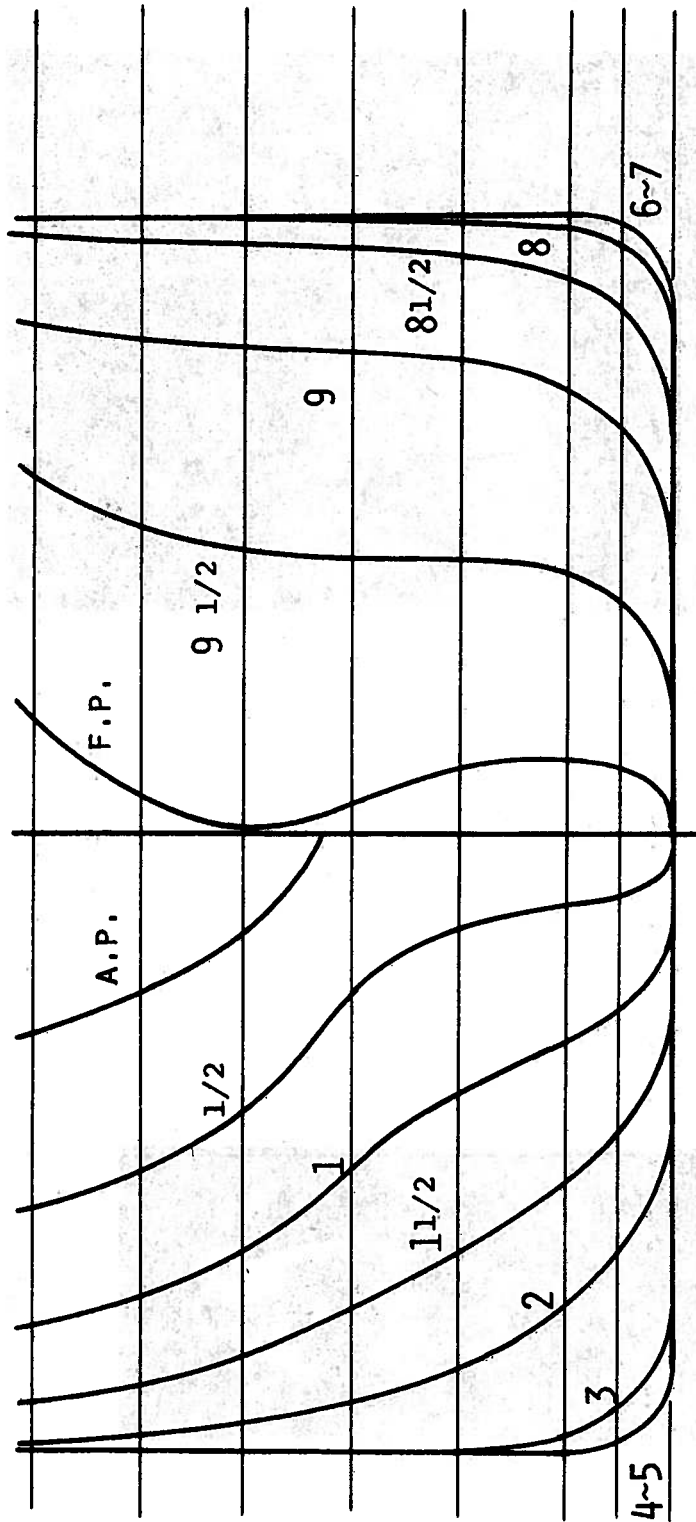


Figure 1. Body plan of the model

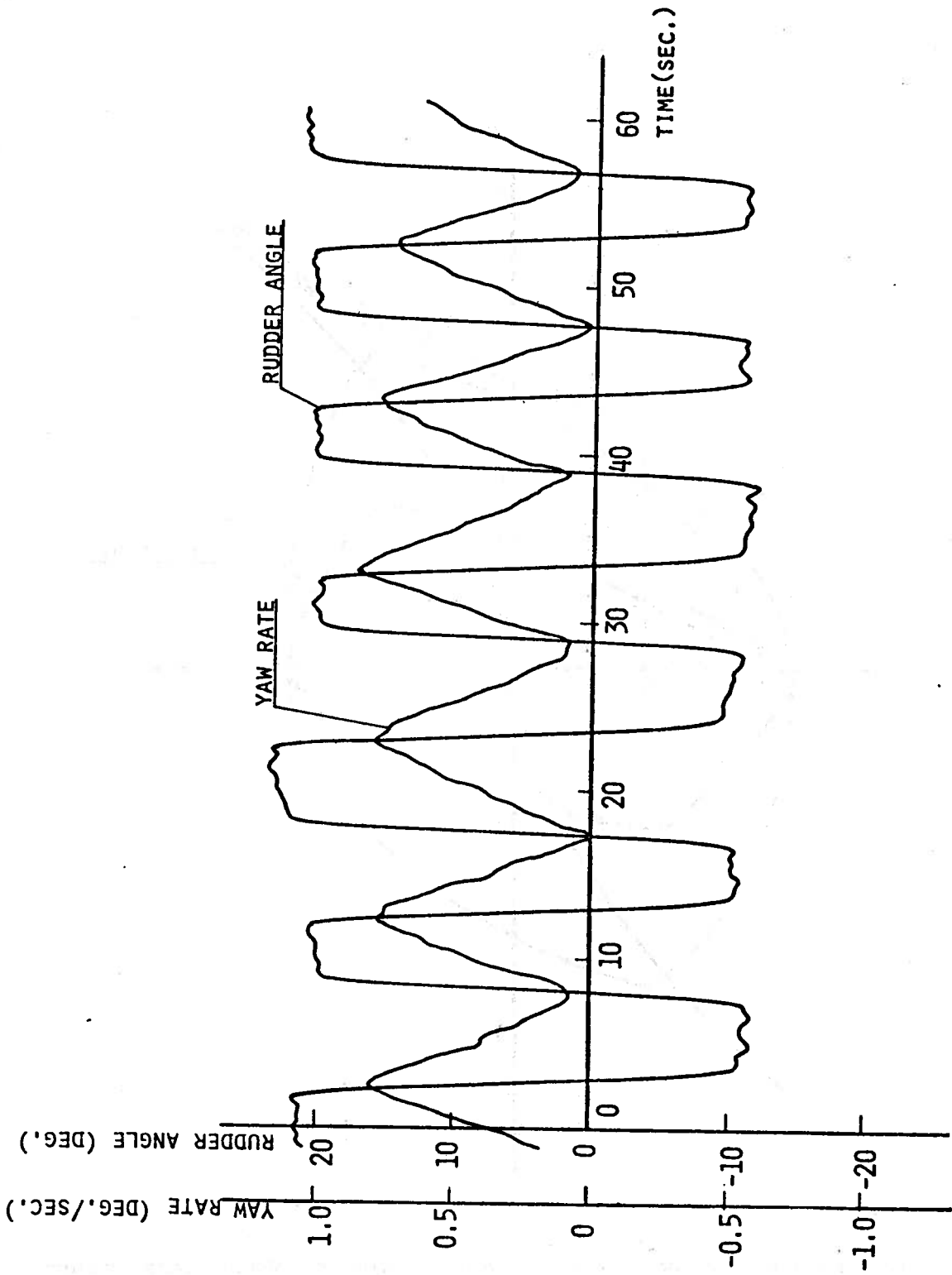


Figure 2. An Example of the time histories of rudder angle and yaw rate recorded at a reversed spiral test ( $H/T=8.7$ , "low" speed)

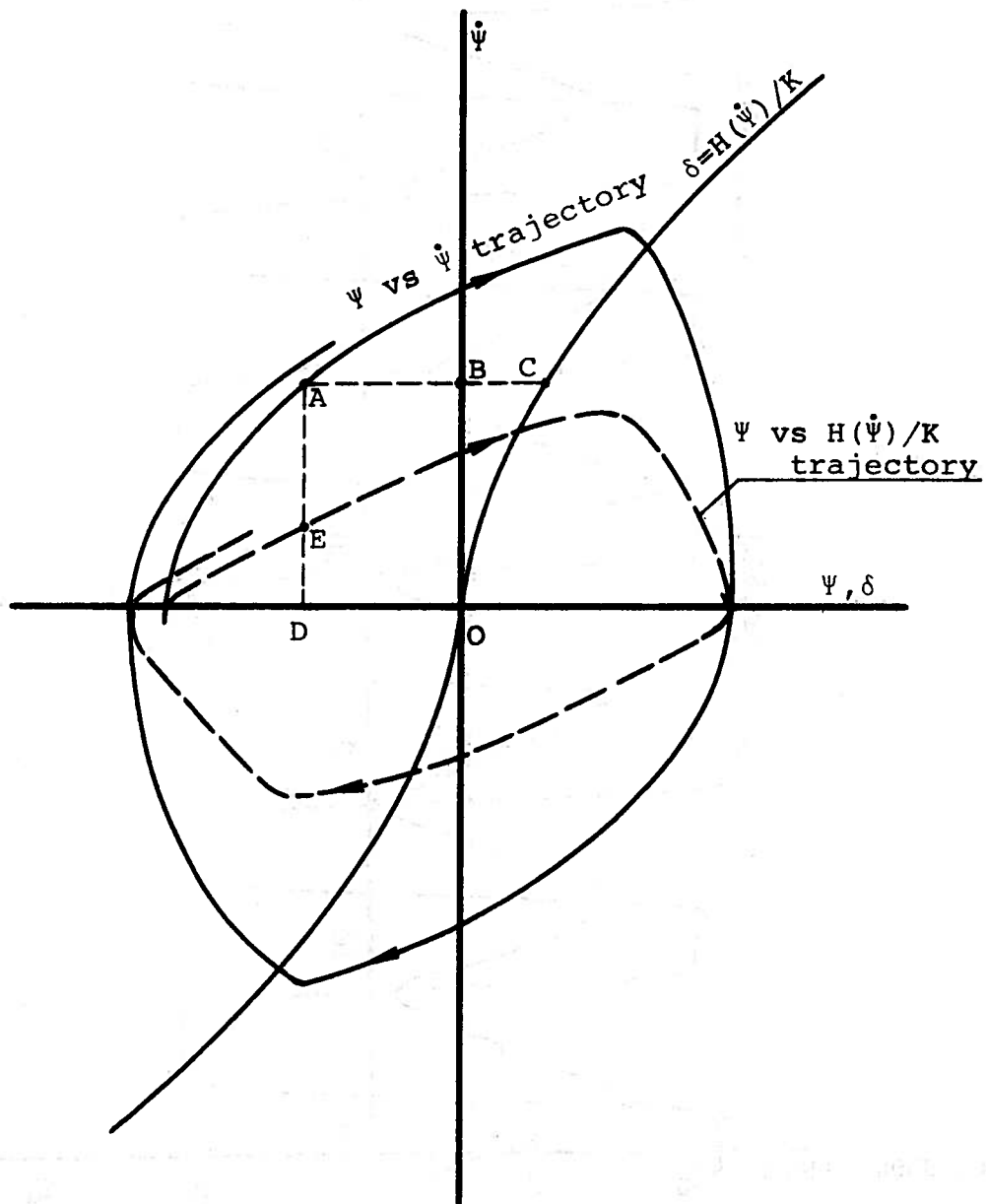


Figure 3. Process of drawing the  $\psi$  versus  $H(\dot{\psi})/K$  phase plane trajectory

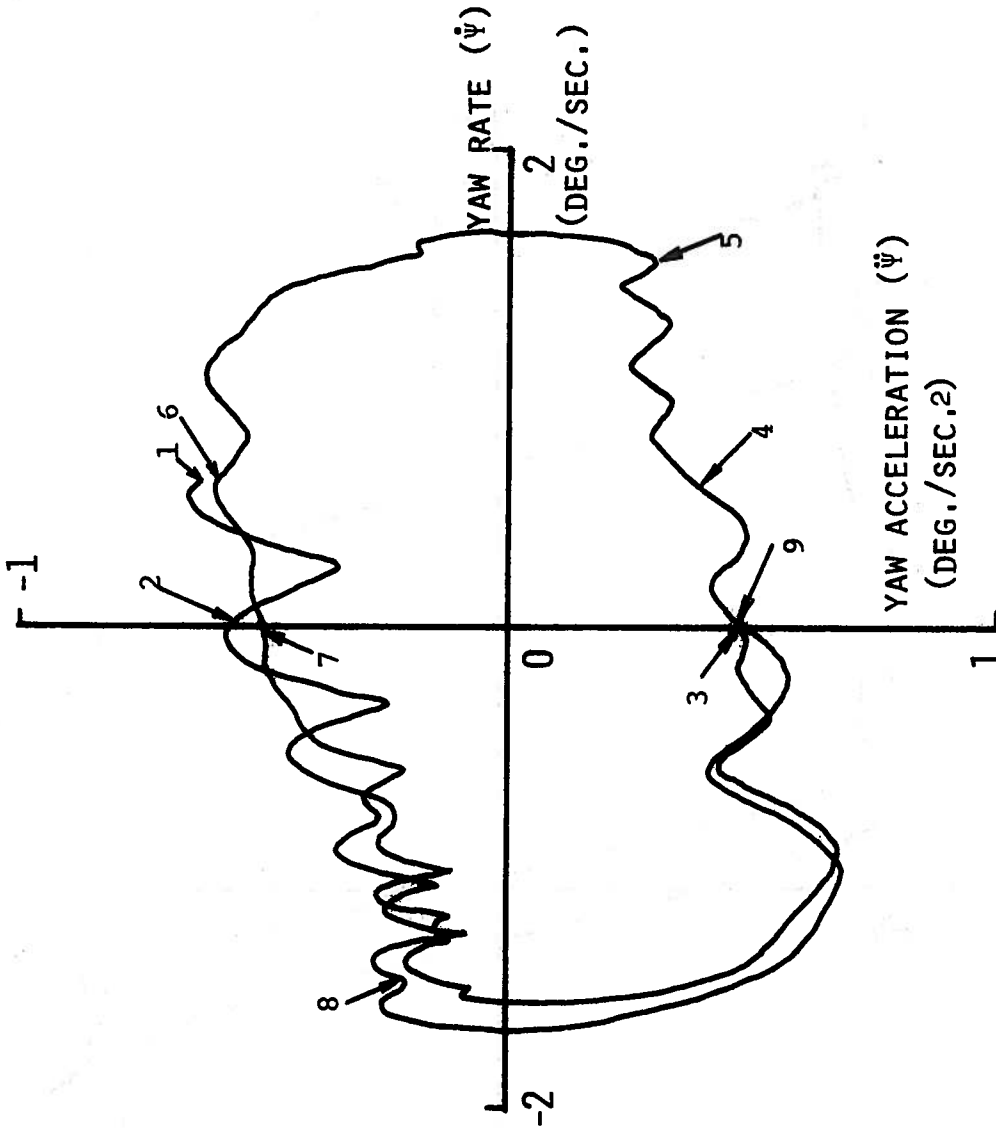


Figure 4. Examples of the various kinds of phase plane trajectories ( $H/T=8.7$ , "medium" speed)  
 a)  $\dot{\psi}$  versus  $\ddot{\psi}$  phase plane trajectory

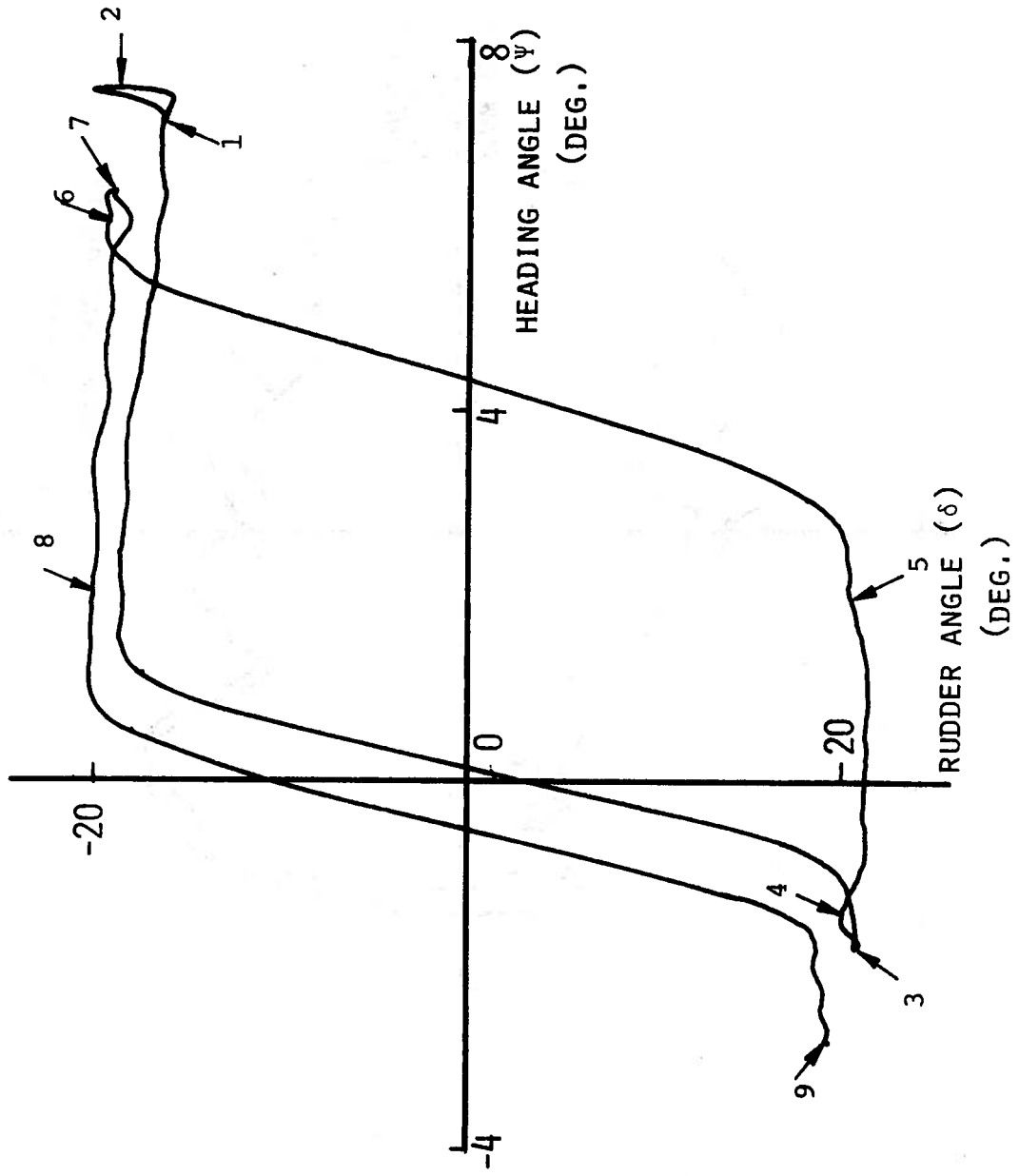


Figure 4. Examples of the various kinds of phase plane trajectories (H/T=8.7, "medium" speed)  
 b)  $\psi$  versus  $\delta$  phase plane trajectory



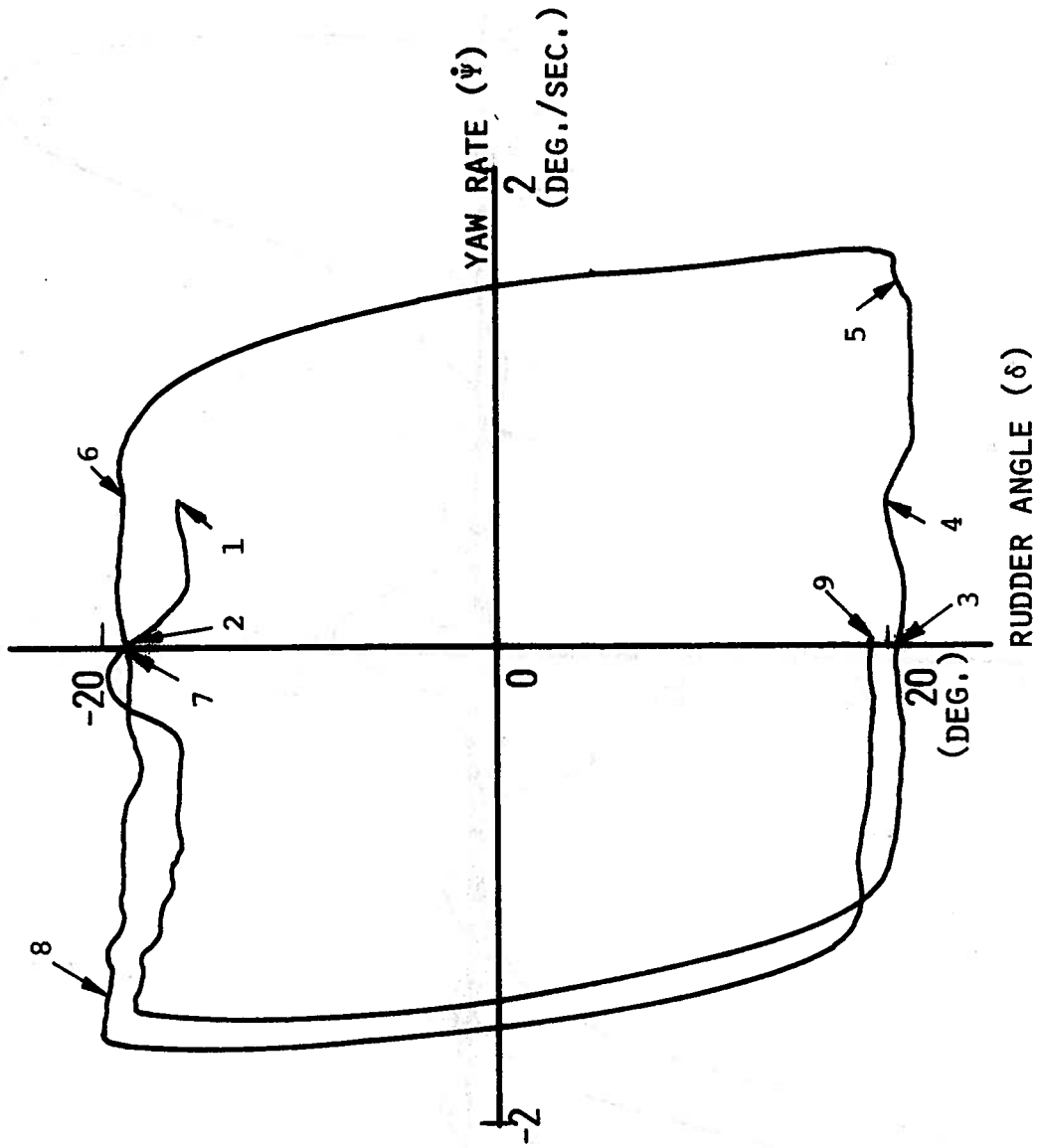


Figure 4. Examples of the various kinds of phase plane trajectories ( $H/T=8.7$ , "medium" speed)  
 c)  $\dot{\psi}$  versus  $\delta$  phase plane trajectory

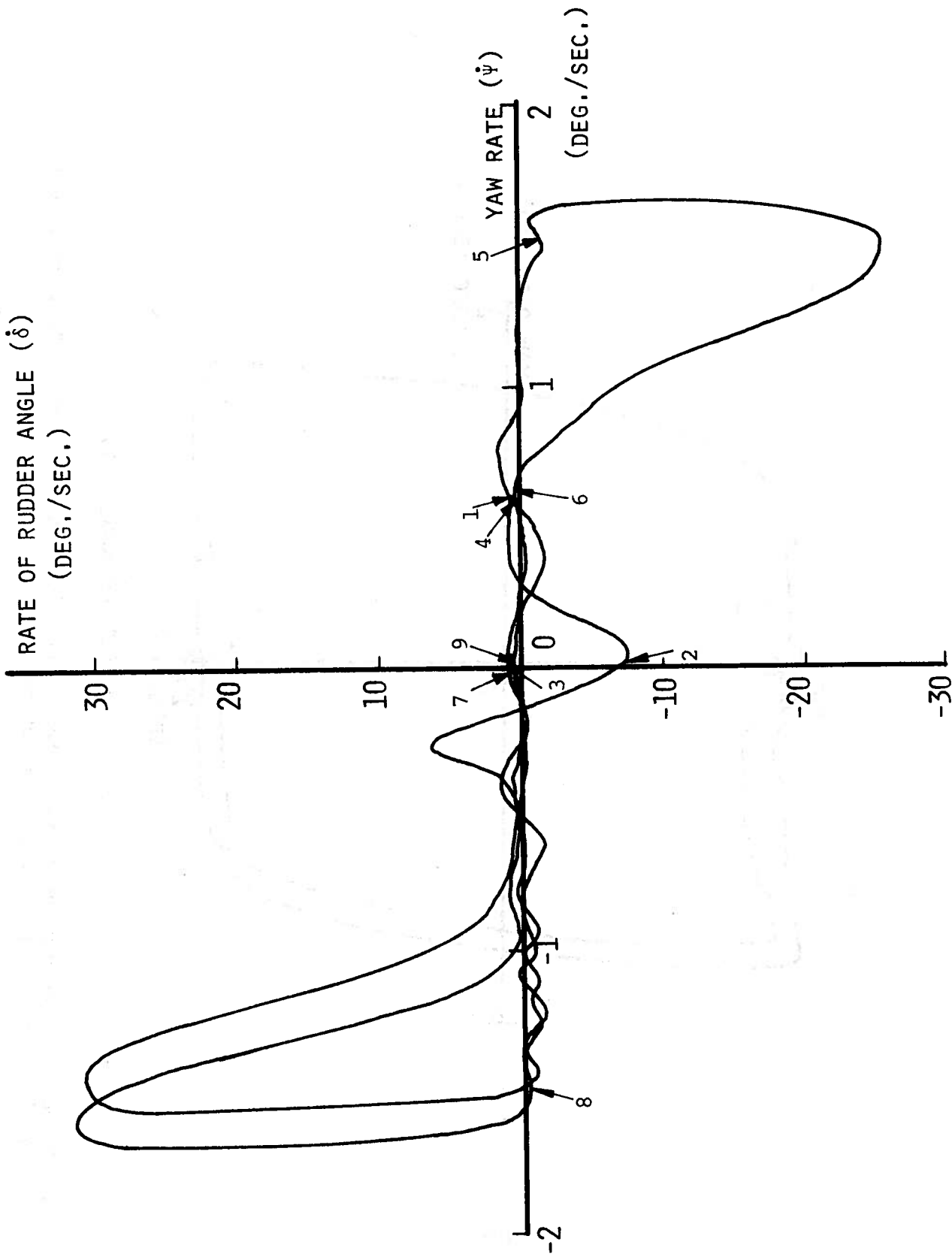


Figure 4. Examples of the various kinds of phase plane trajectories ( $H/T=8.7$ , "medium" speed)  
 d)  $\dot{\psi}$  versus  $\dot{\delta}$  phase plane trajectory

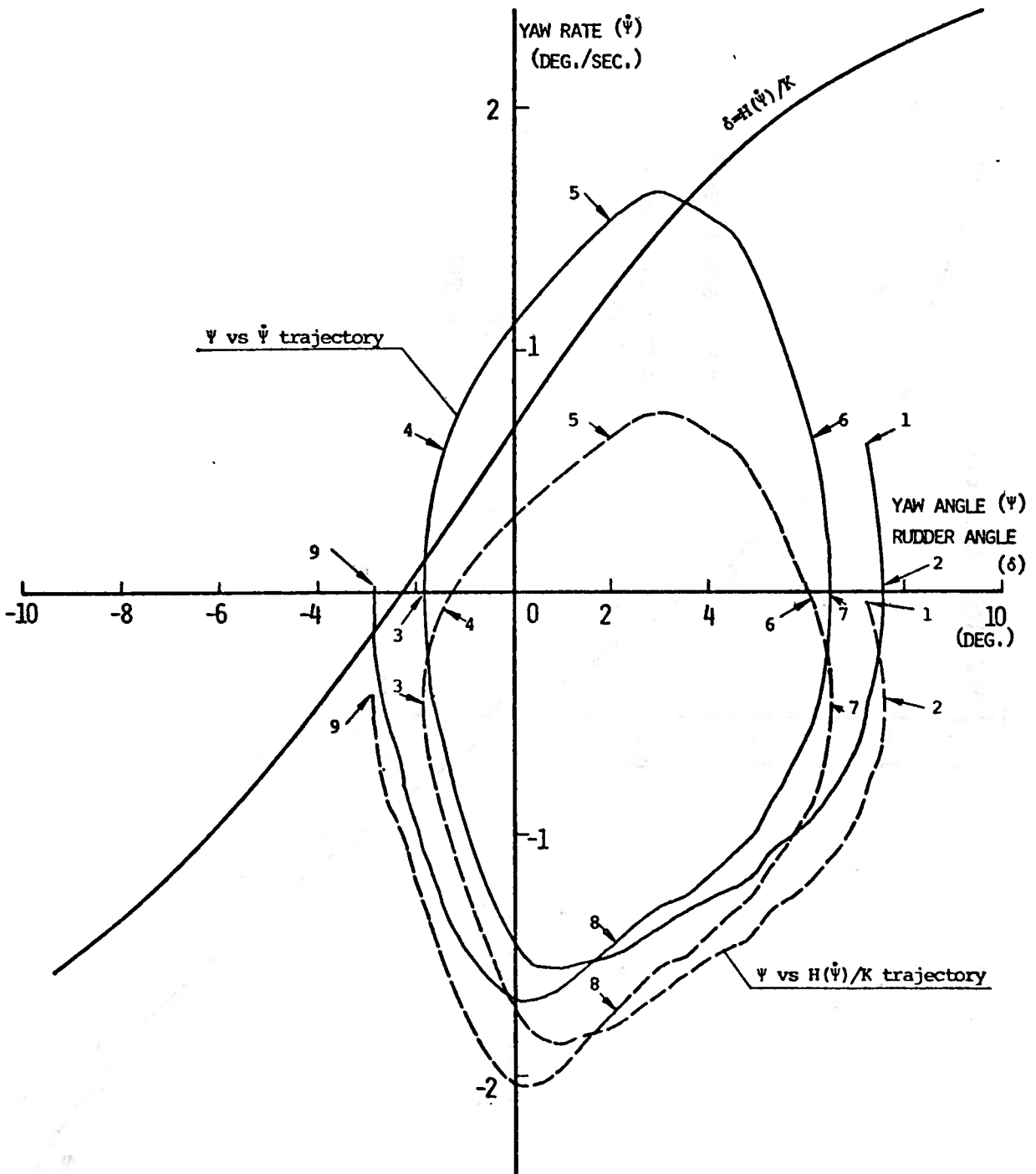


Figure 4. Examples of the various kinds of phase plane trajectories ( $H/T=8.7$ , "medium" speed)  
 e)  $\psi$  versus  $H(\dot{\psi})/K$  phase plane trajectory

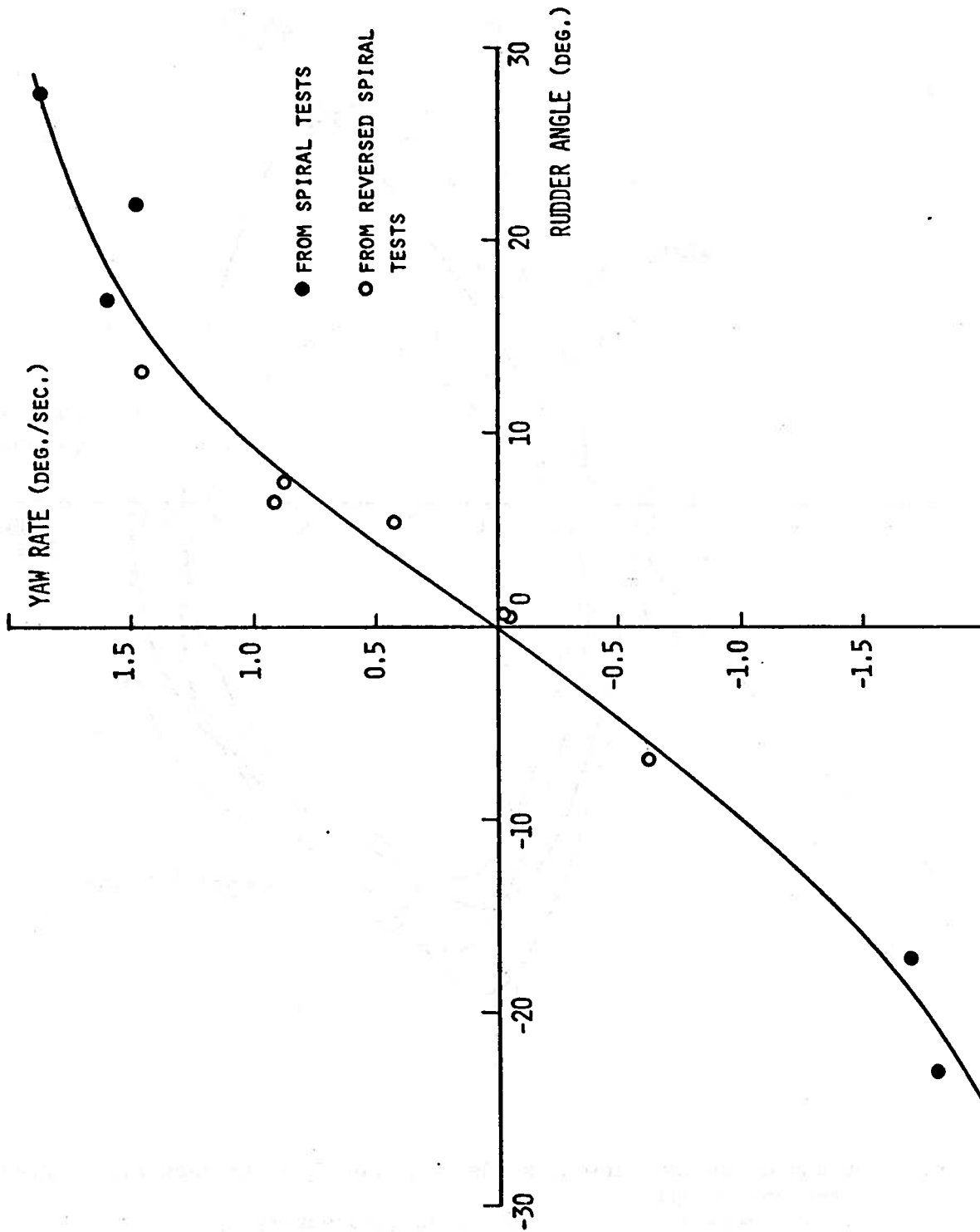


Figure 5. Stationary turning characteristics in case of  $H/T=8.7$  and "low" speed

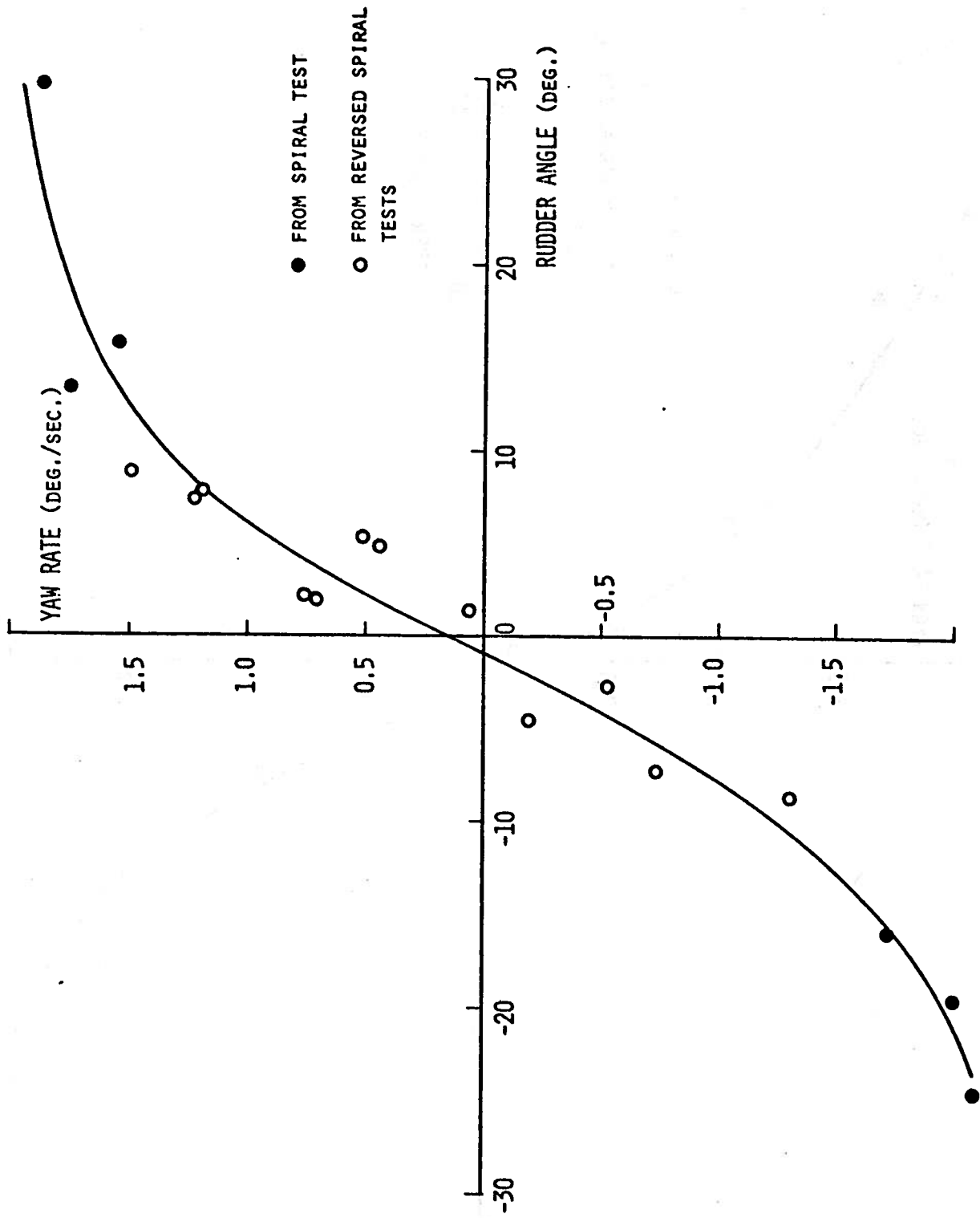


Figure 6. Stationary turning characteristics in case of  $H/T=3.0$  and "low" speed

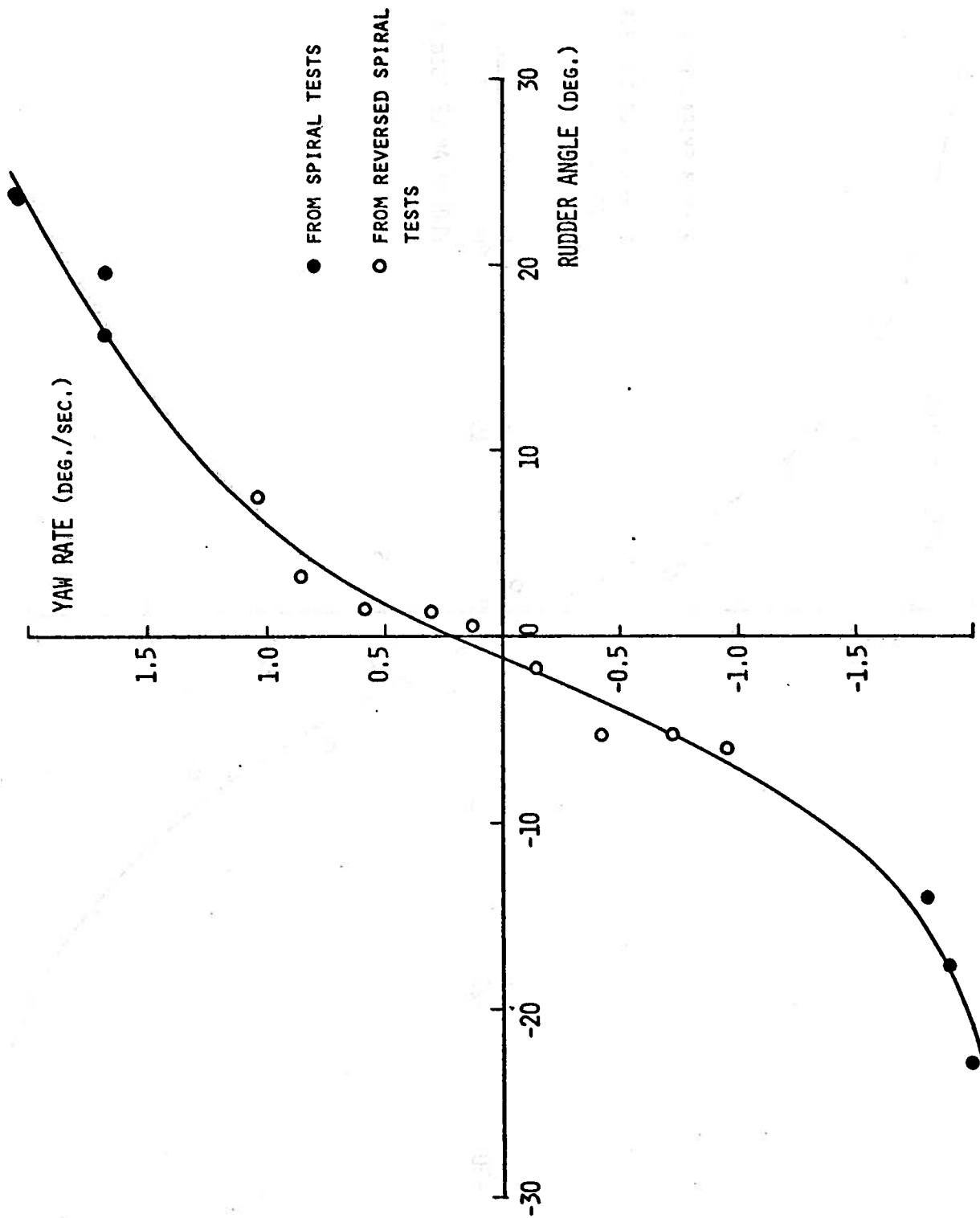


Figure 7. Stationary turning characteristics in case of  $K/T=2.0$  and "low" speed

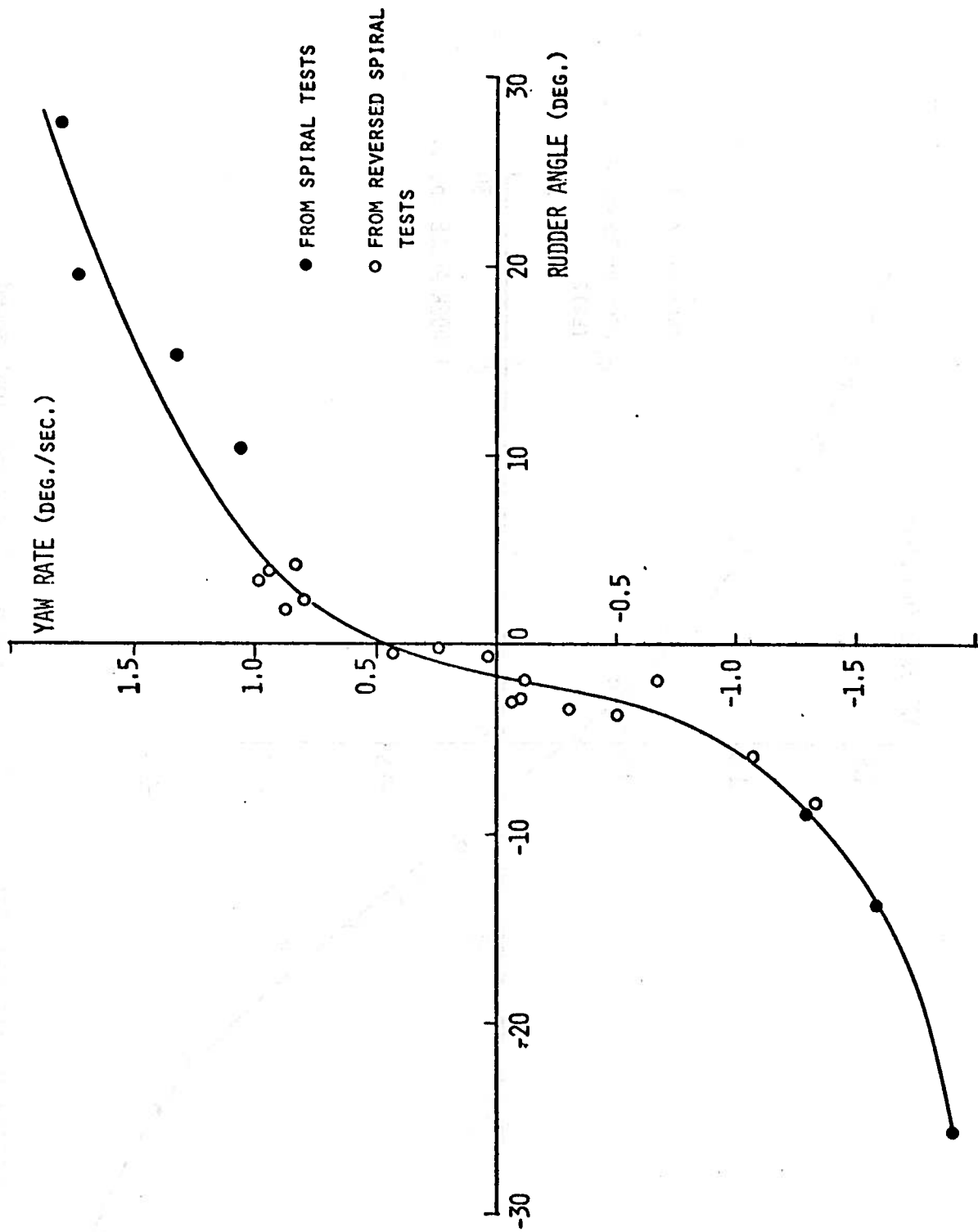


Figure 8. Stationary turning characteristics in case of  $H/T=1.5$  and "low" speed

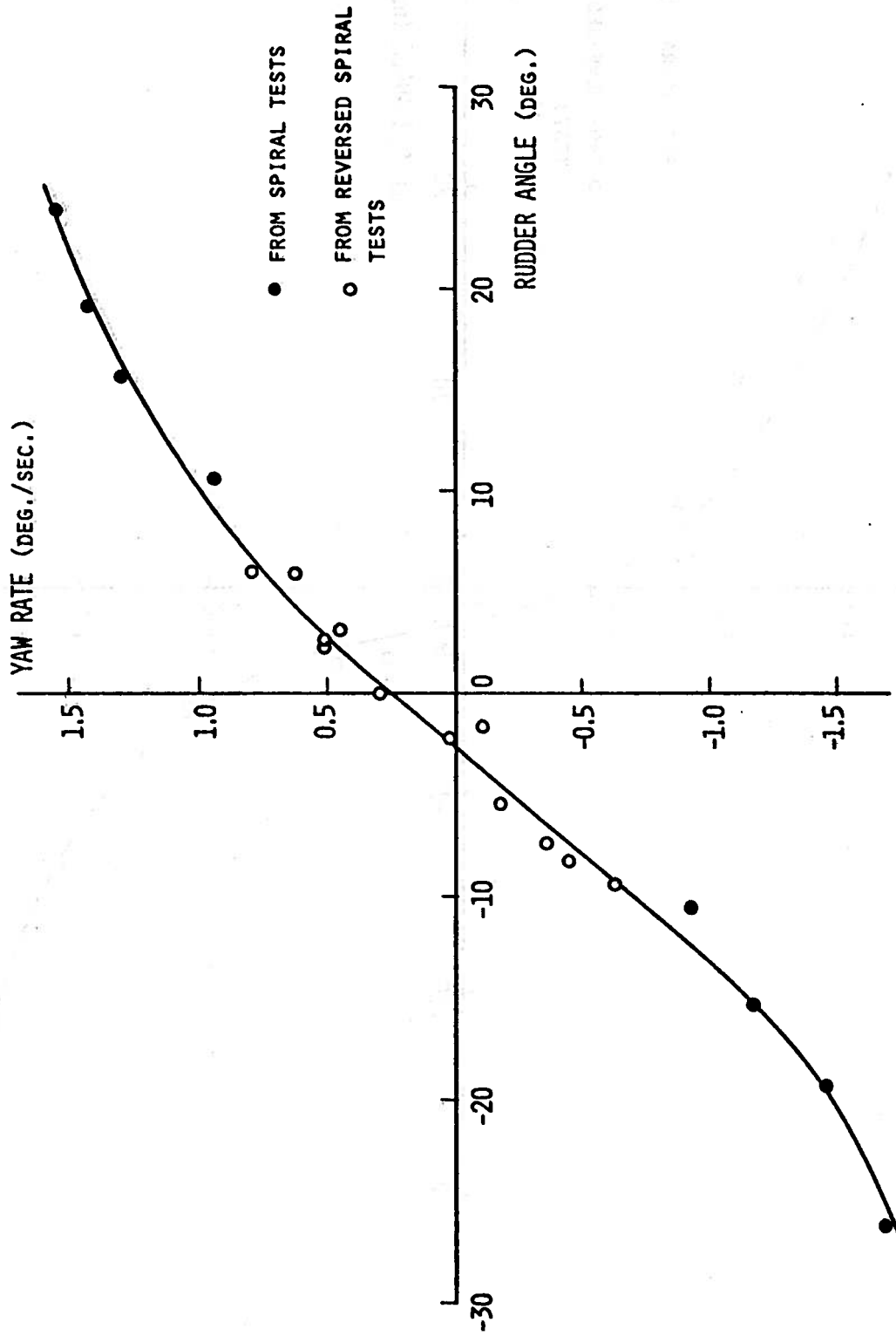


Figure 9. Stationary turning characteristics in case of  $H/T=1.2$  and "low" speed



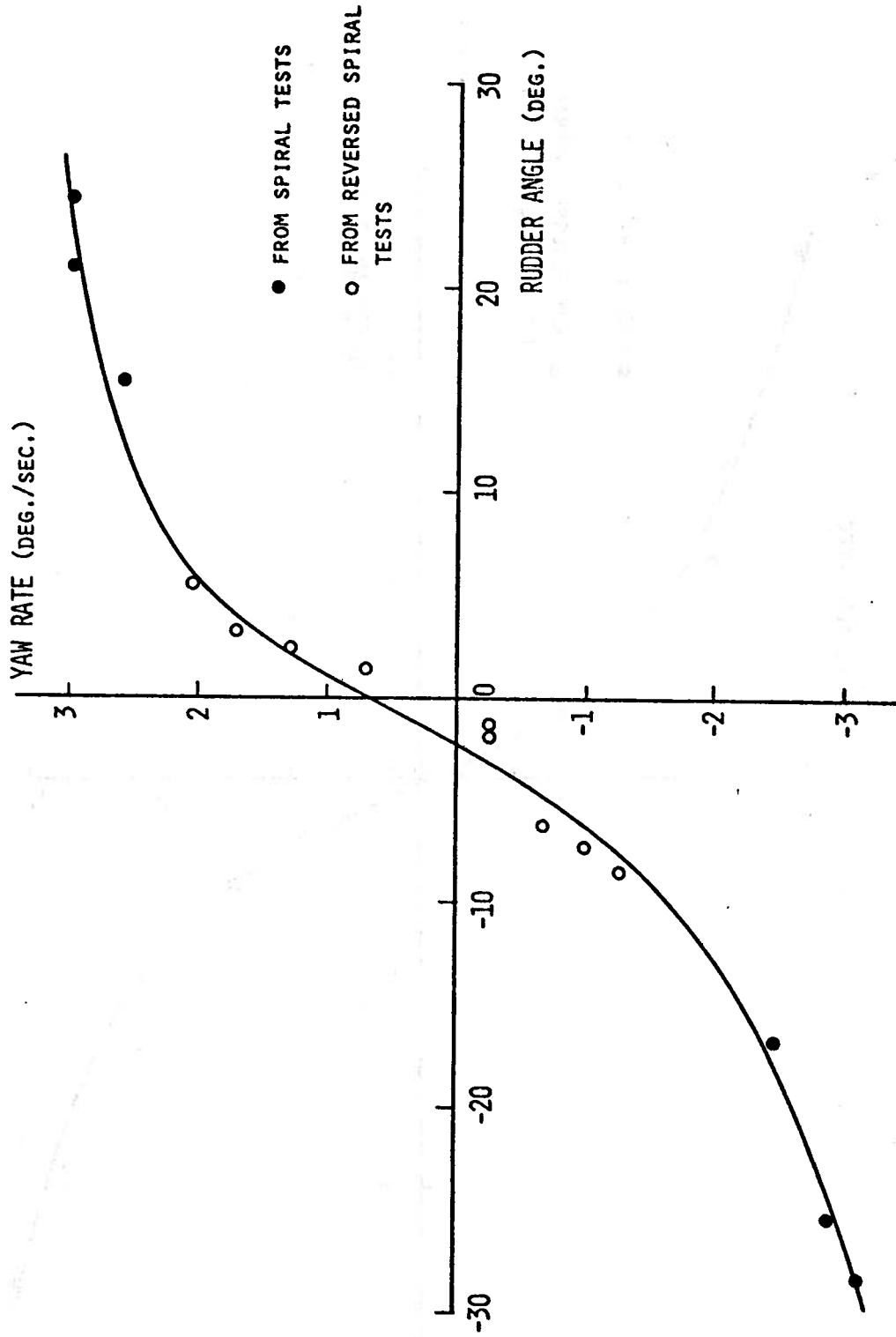


Figure 10. Stationary turning characteristics in case of  $H/T=8.7$  and "medium" speed

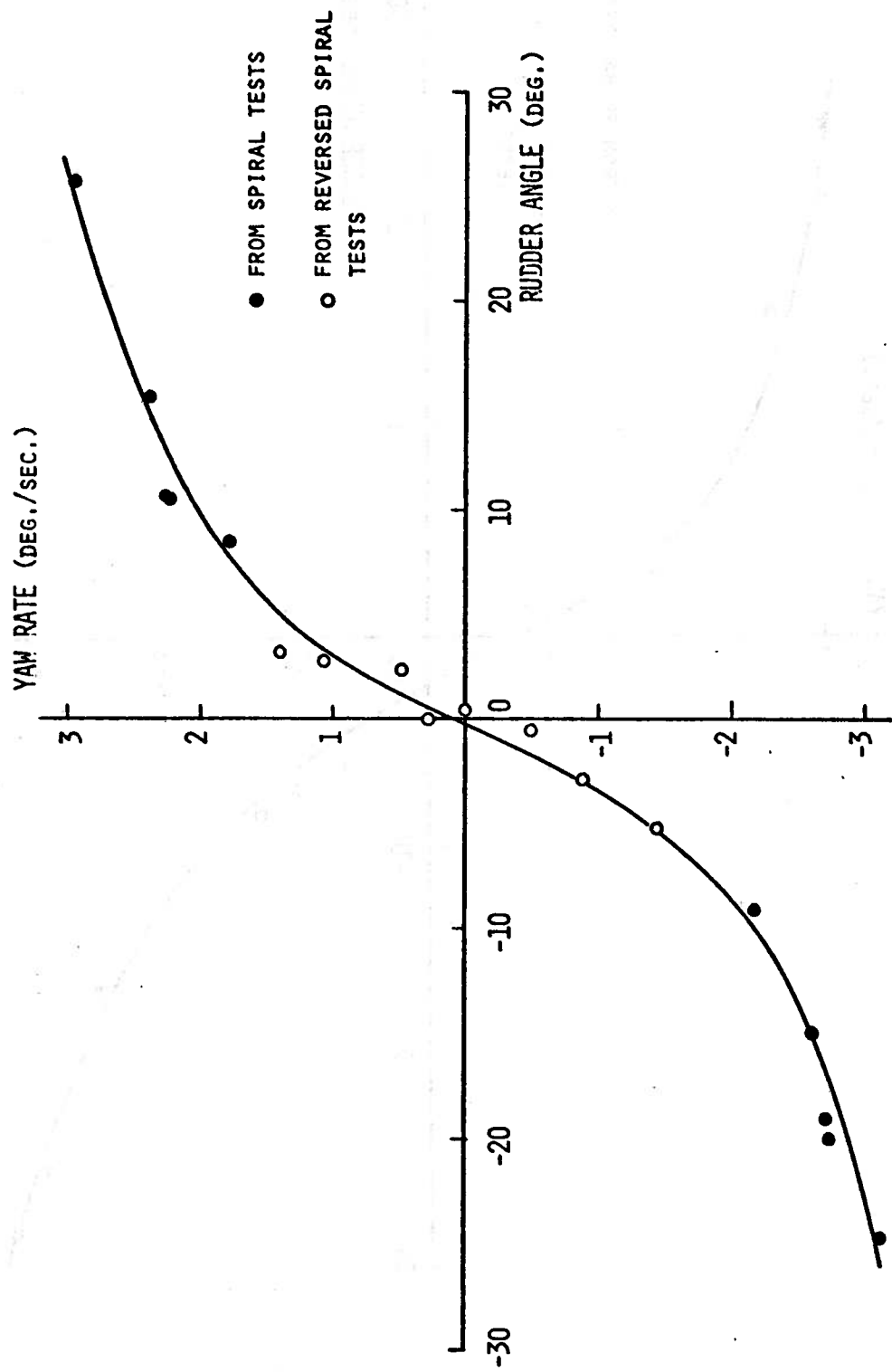


Figure 11. Stationary turning characteristics in case of  $H/T=3.0$  and "medium" speed

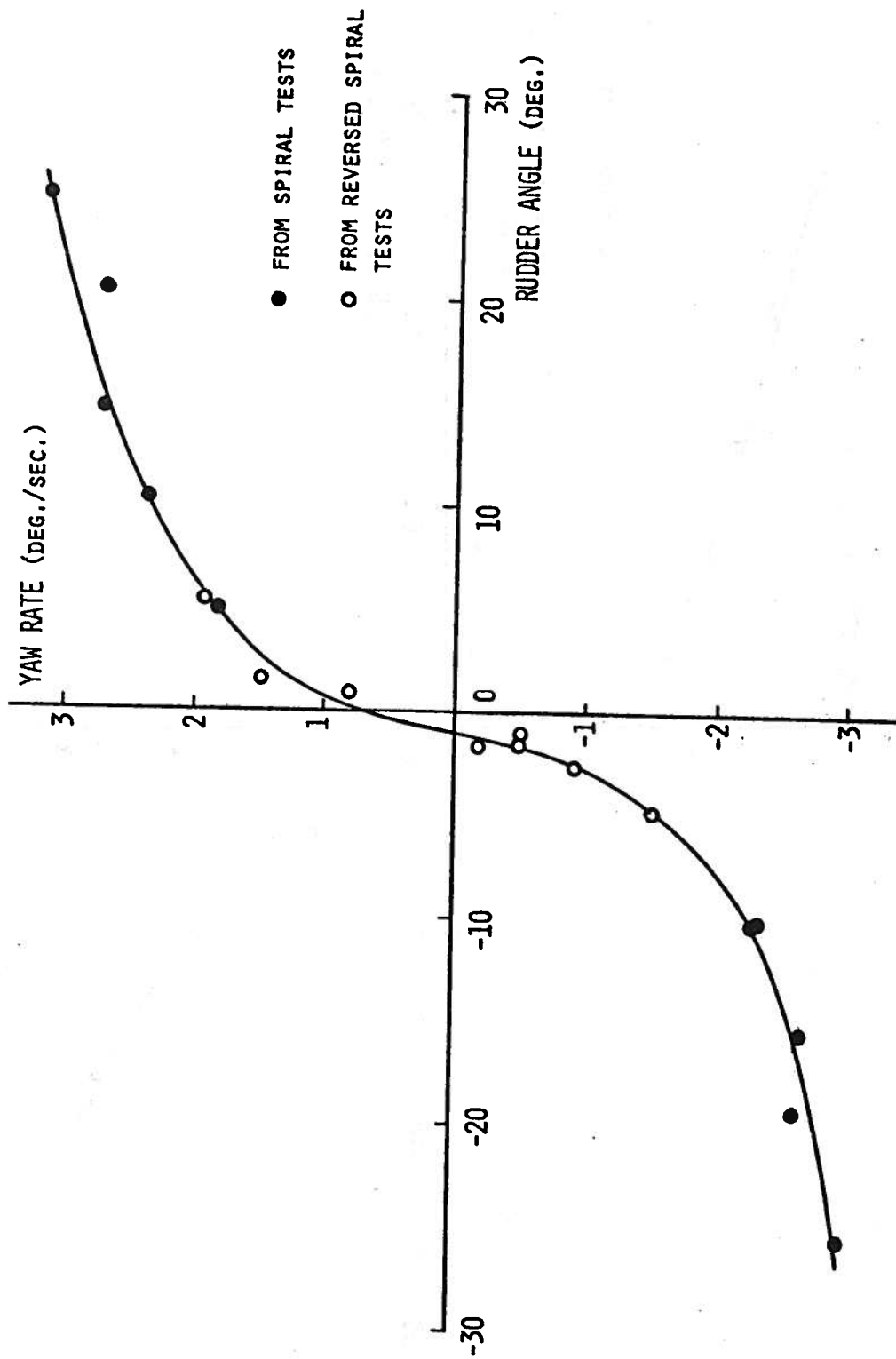


Figure 12. Stationary turning characteristics in case of  $H/T=2.0$  and "medium" speed

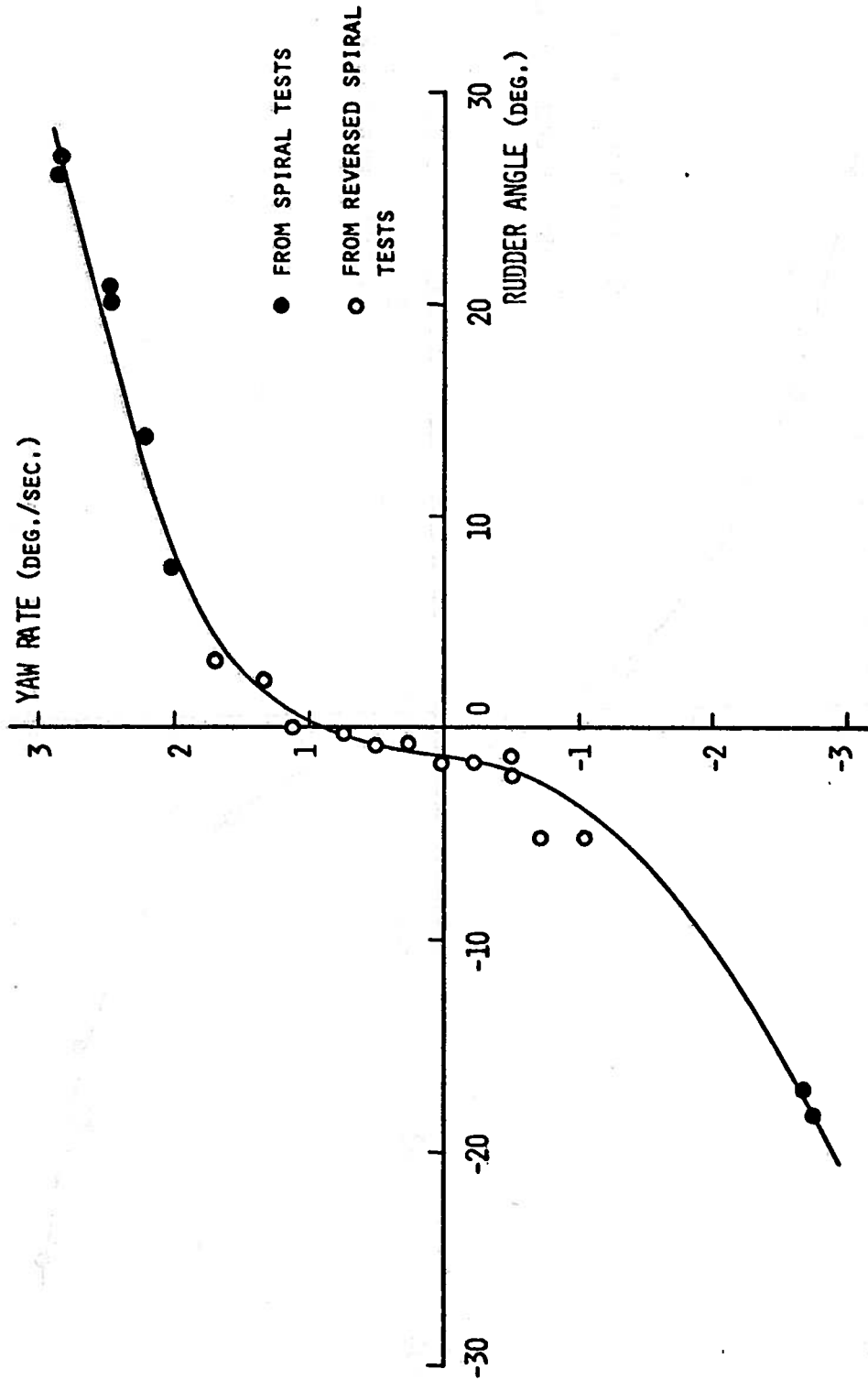


Figure 13. Stationary turning characteristics in case of H/T=1.5 and "medium" speed

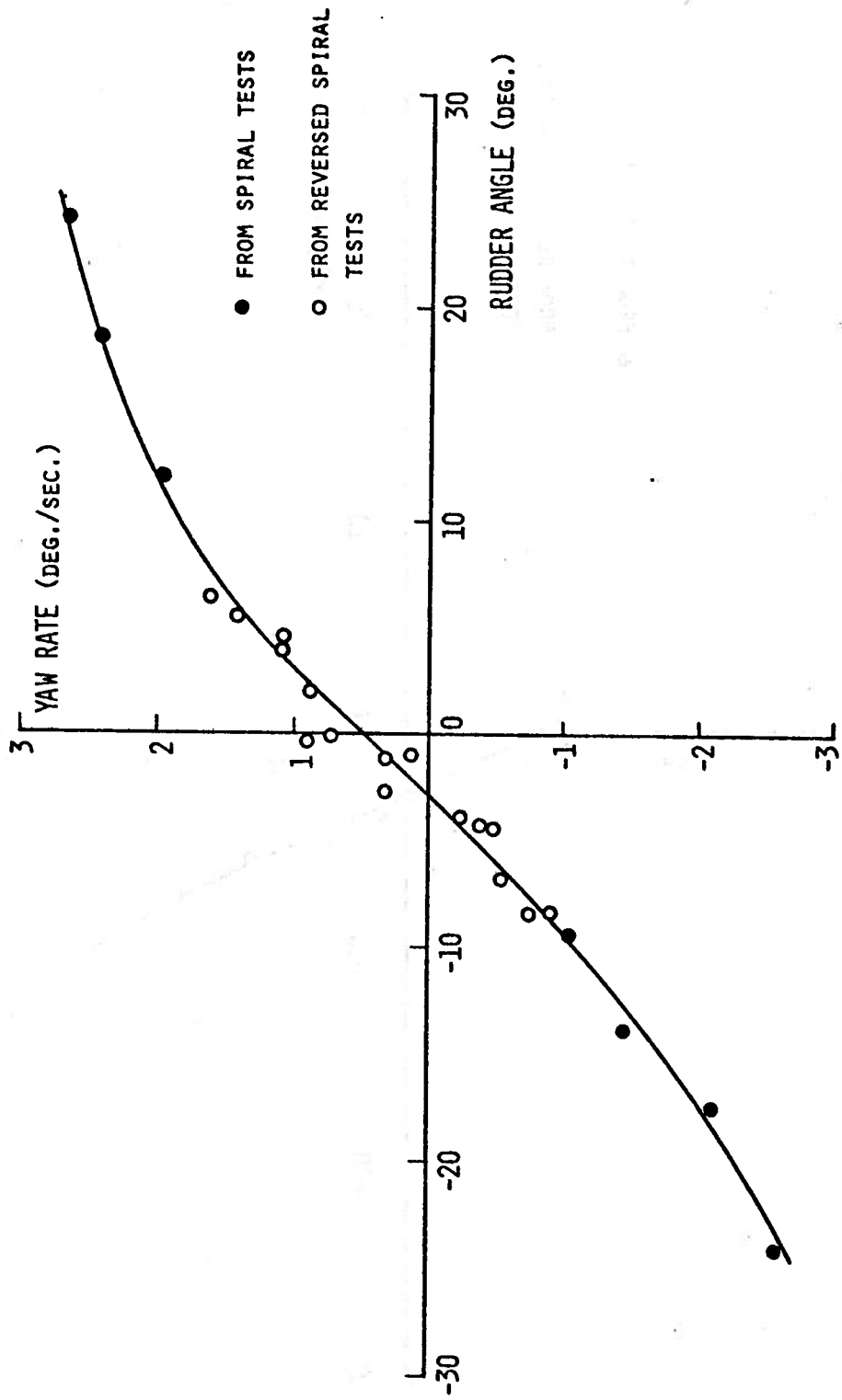


Figure 14. Stationary turning characteristics in case of H/T=1.2 and "medium" speed

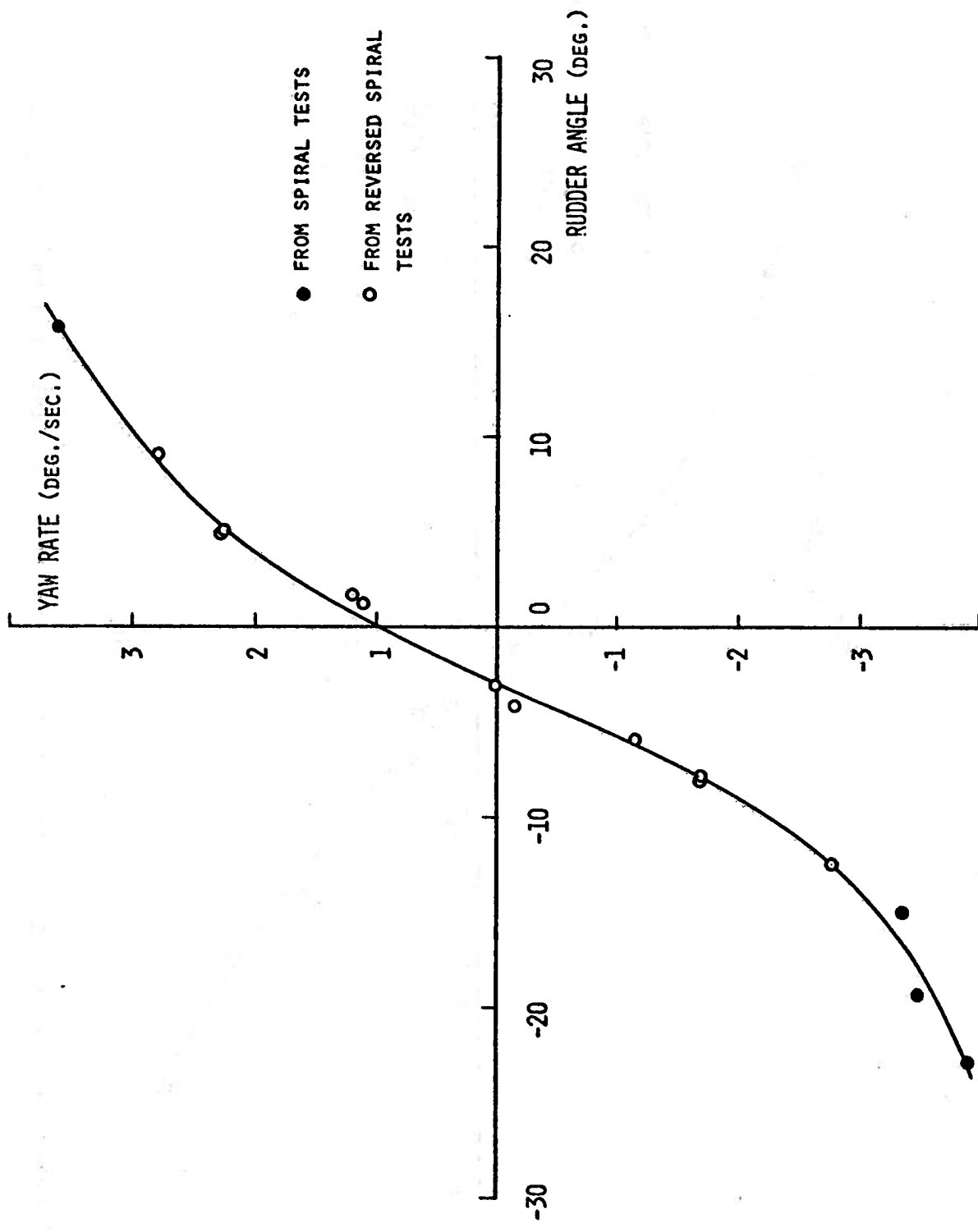


Figure 15. Stationary turning characteristics in case of  $H/T=8.7$  and "high" speed

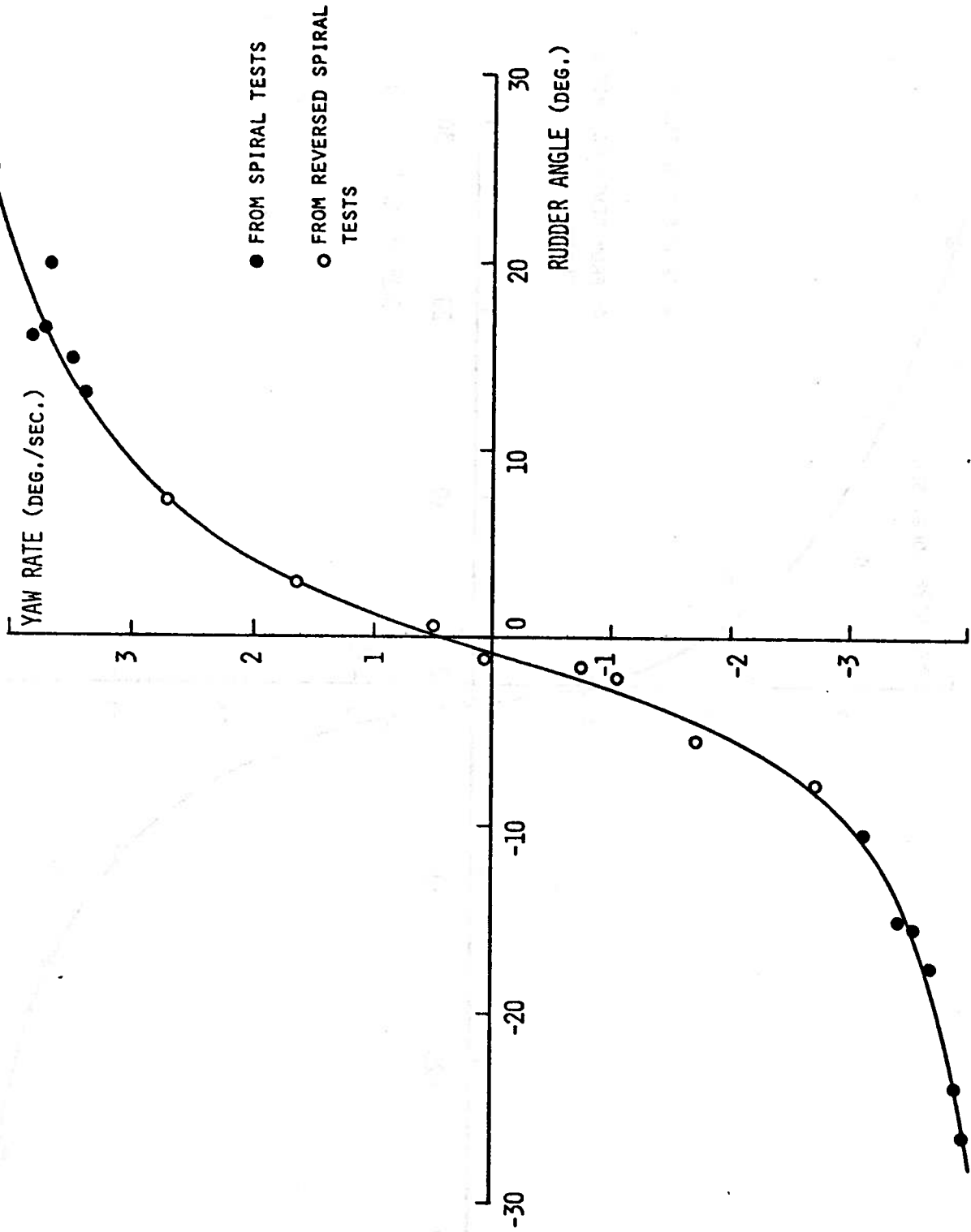


Figure 16. Stationary turning characteristics in case of H/T=3.0 and "high" speed

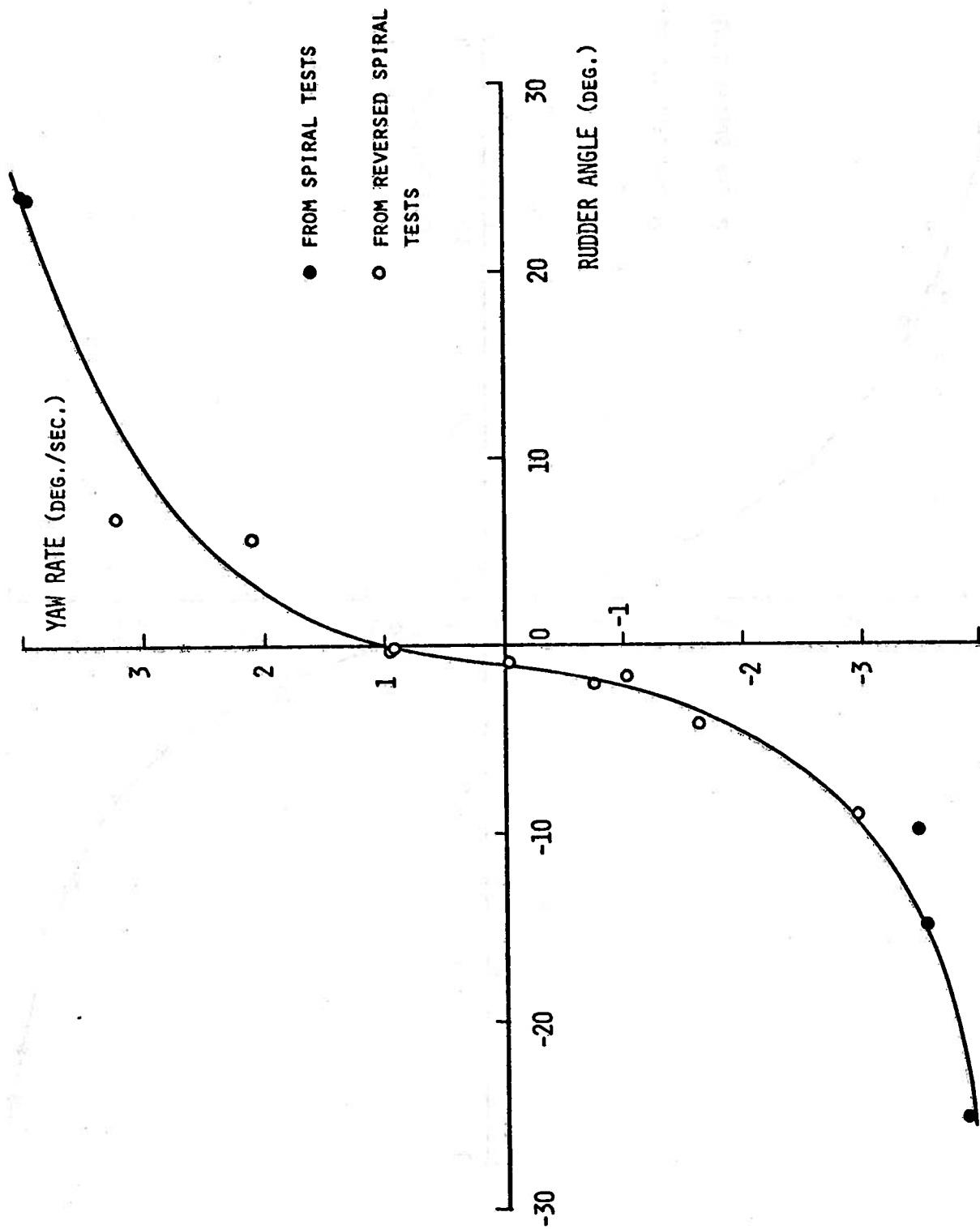


Figure 17. Stationary turning characteristics in case of H/T=2.0 and "high" speed



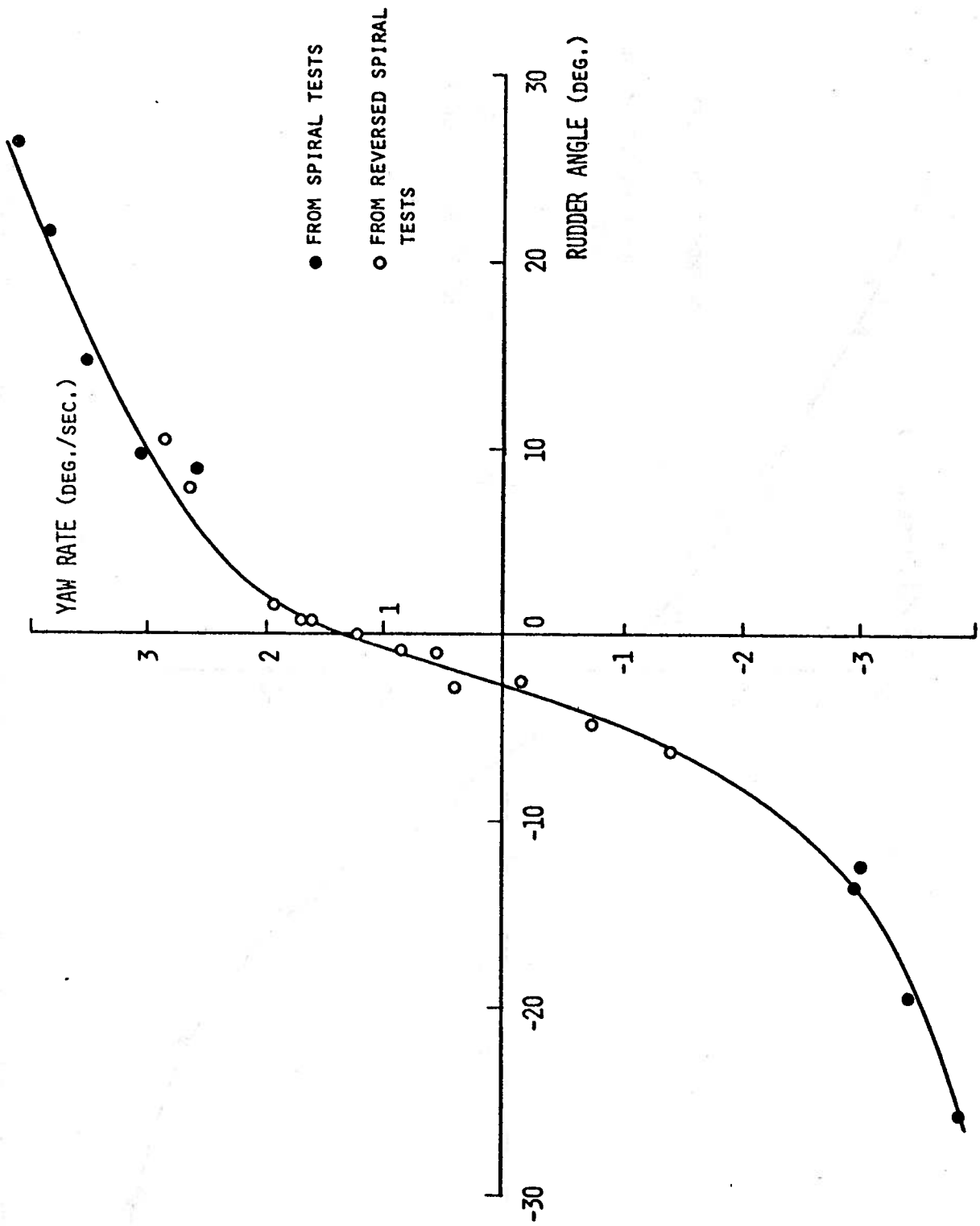


Figure 18. Stationary turning characteristics in case of  $H/T=1.5$  and "high" speed

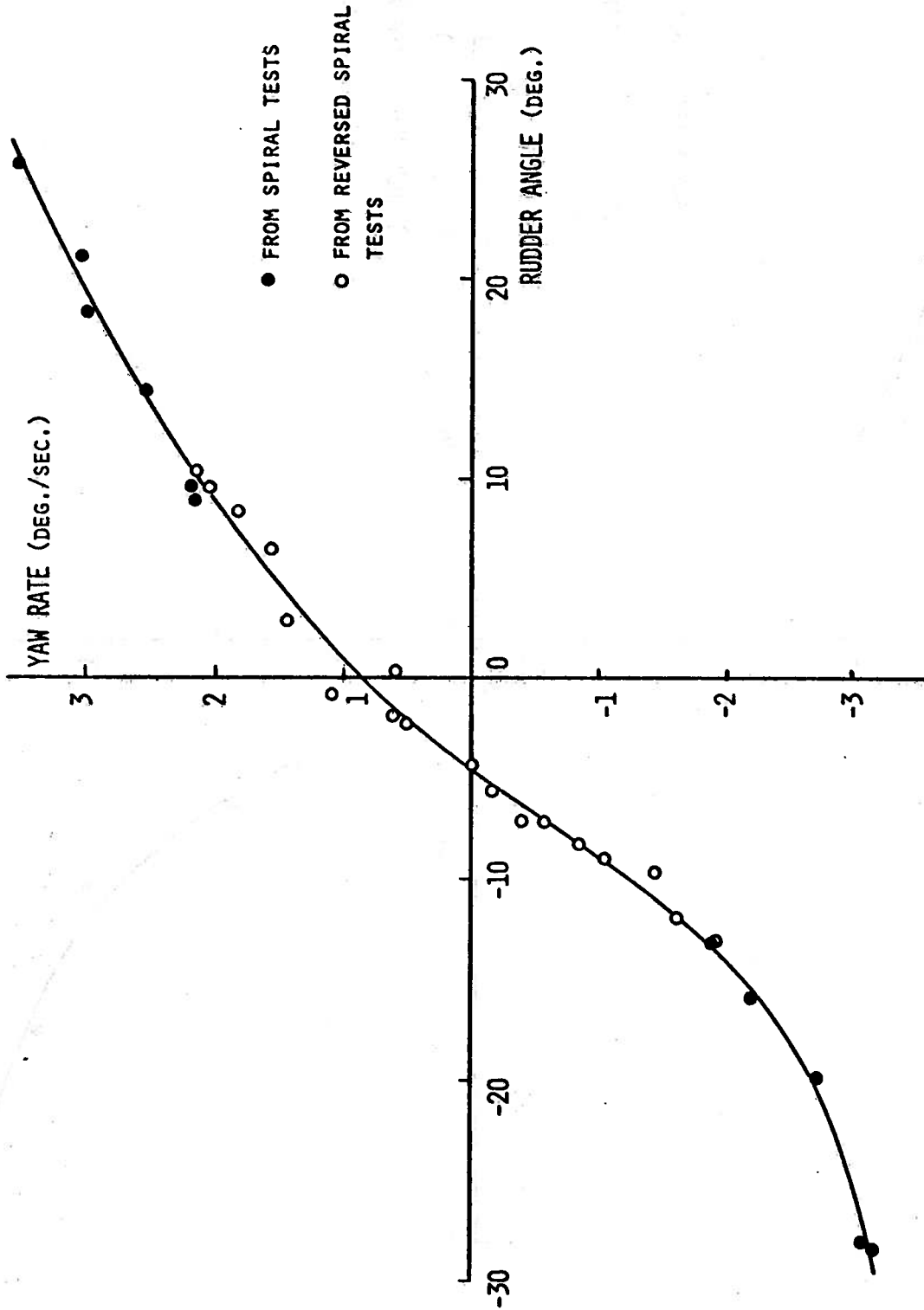


Figure 19. Stationary turning characteristics in case of  $H/T=1.2$  and "high" speed

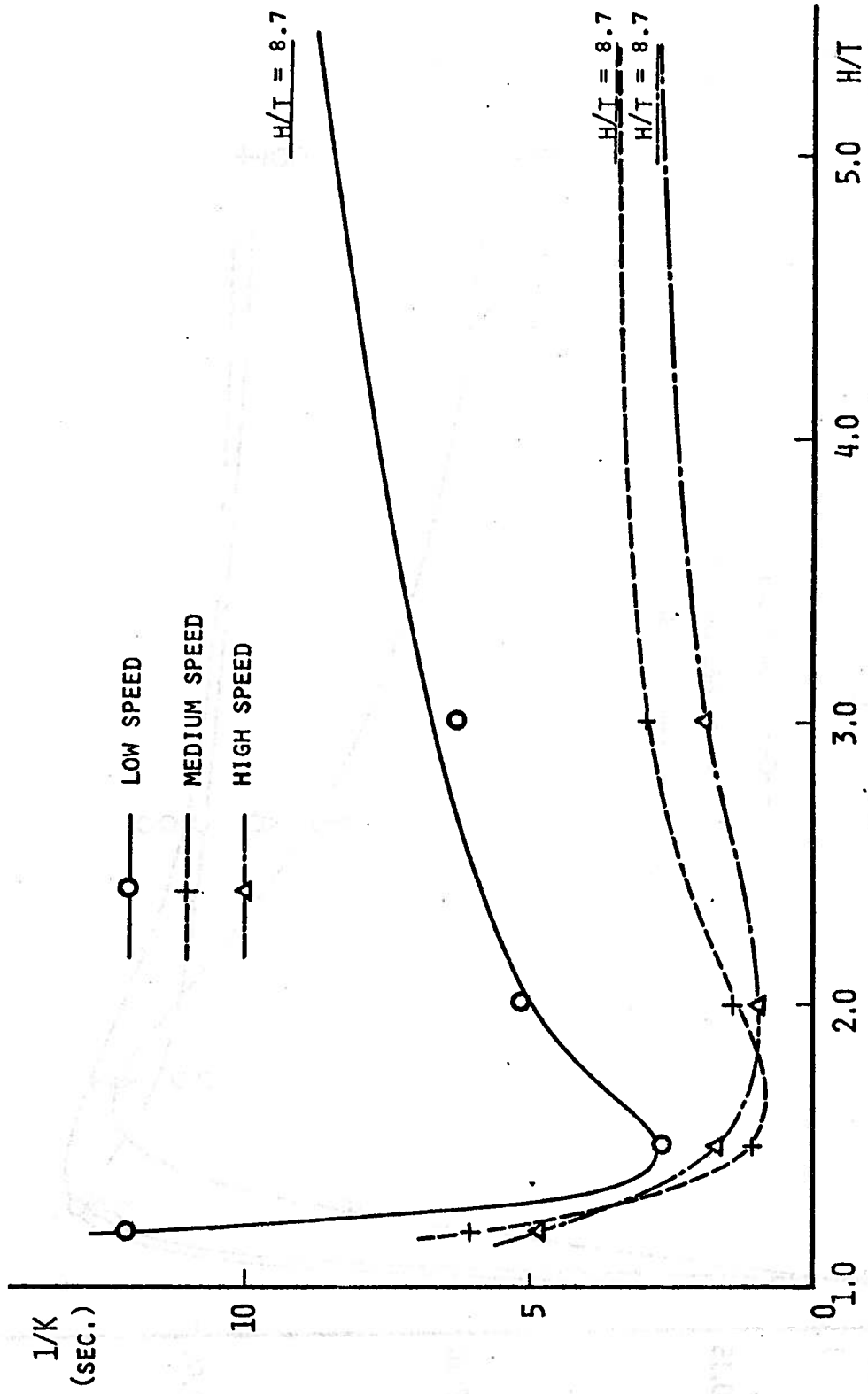


Figure 20. K index versus water-depth/draft ratio relationship for different model speed

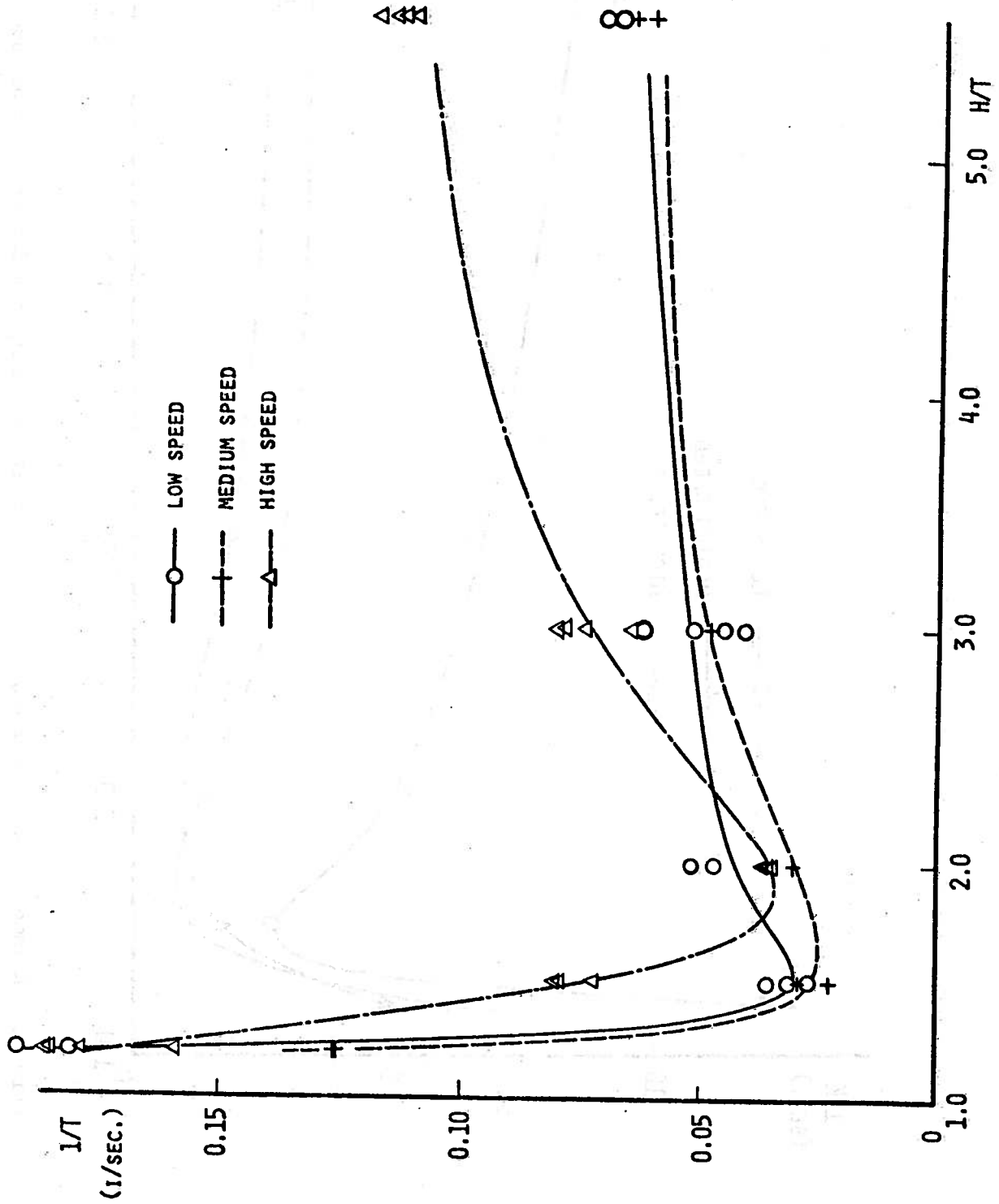


Figure 21. T1 index versus water-depth/draft ratio relationship for different model speed

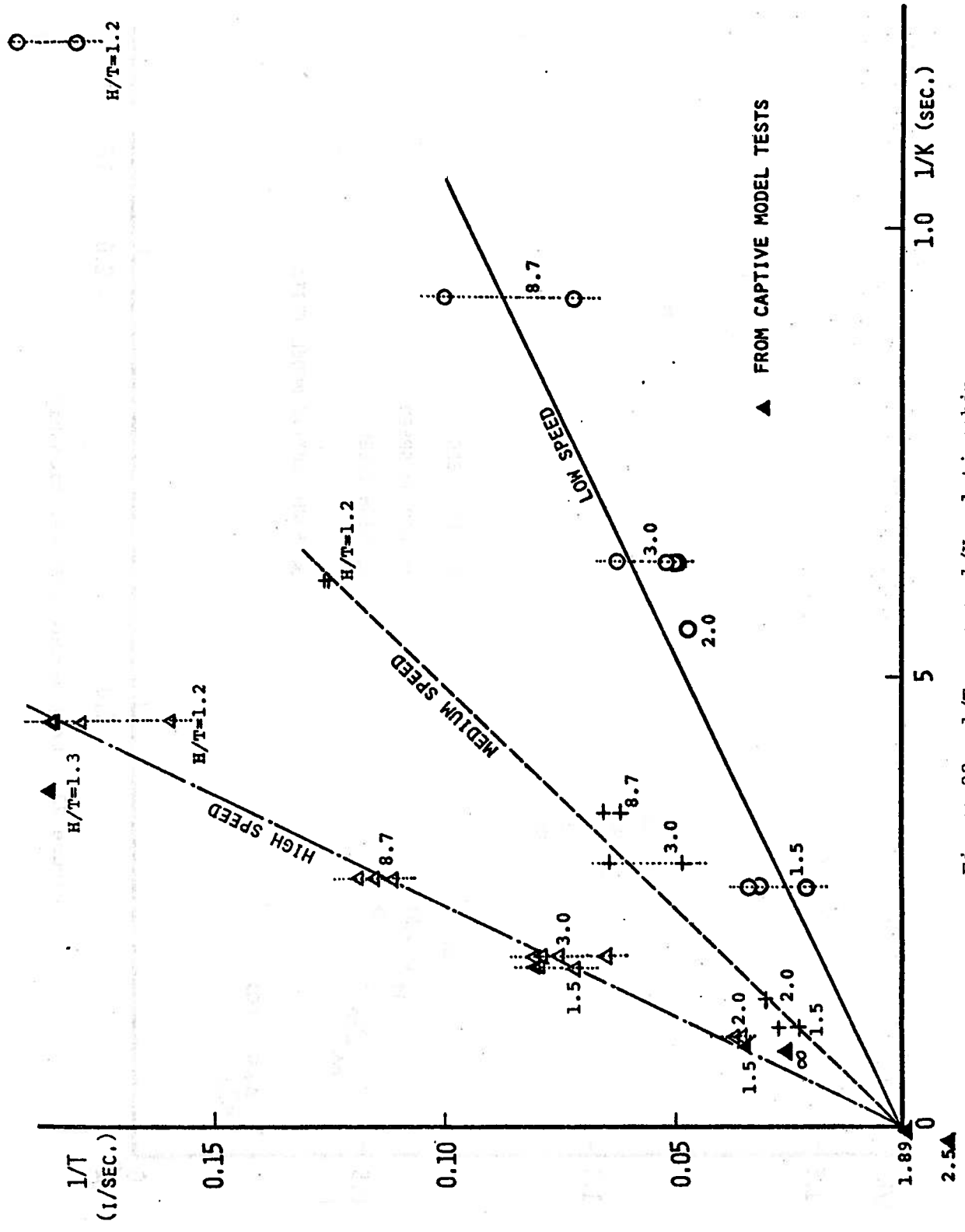


Figure 22.  $1/T_1$  versus  $1/K$  relationship

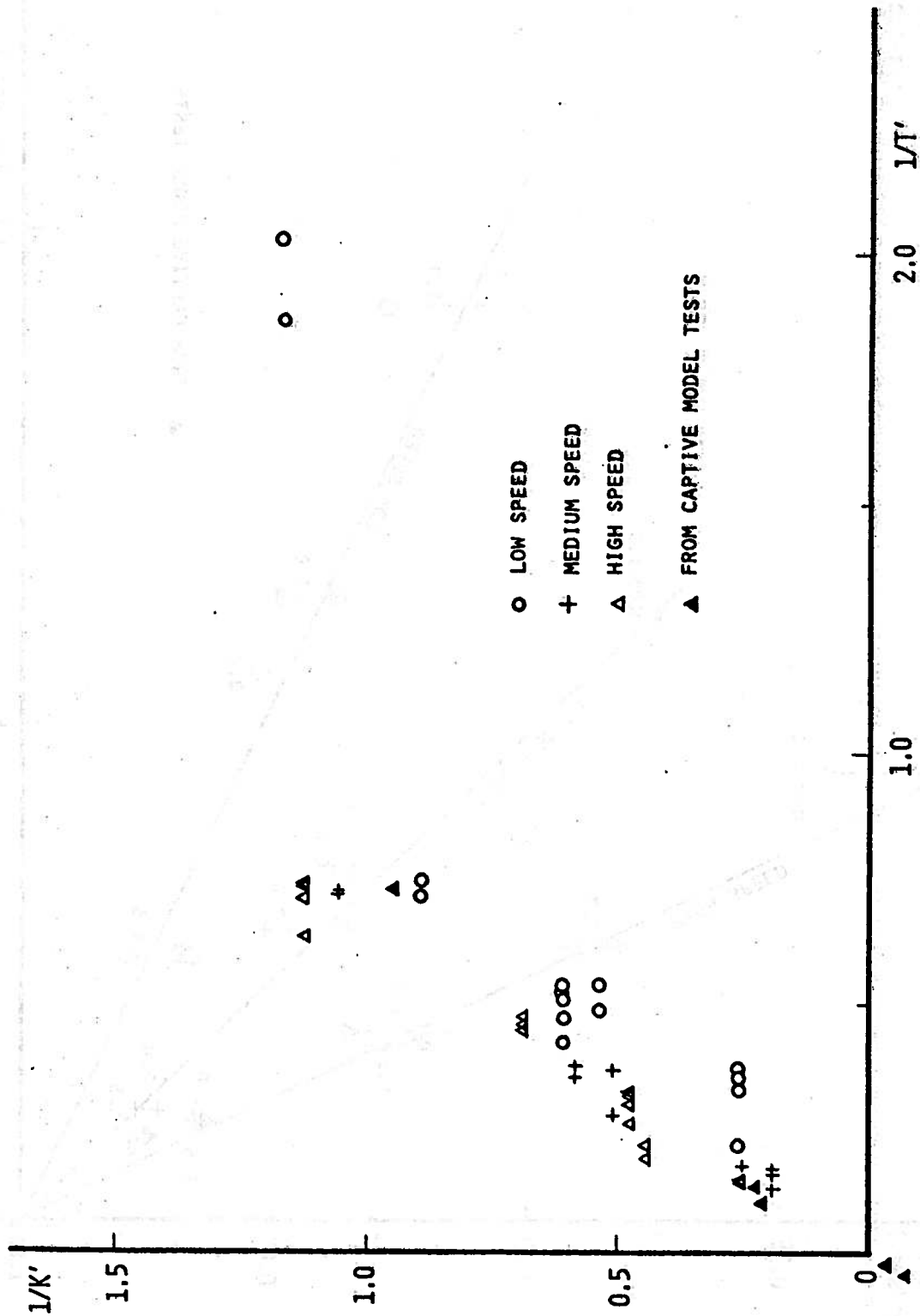



Figure 23. 1/Tl versus 1/K' relationship

 The University of Michigan is an equal opportunity/affirmative action employer. Under applicable federal and state laws, including Title IX of the Education Amendments of 1972, the University does not discriminate on the basis of sex, race, or other prohibited matters in employment, in educational programs and activities, or in admissions. Inquiries or complaints may be addressed to the University's Director of Affirmative Action and Title IX Compliance: Dr. Gwendolyn C. Baker, 5072 Administration Building, 763-0235.